# A SMOOTH TRANSITION MODEL BETWEEN KINETIC AND HYDRODYNAMIC EQUATIONS

Pierre Degond[1], Shi Jin[2], Luc Mieussens[1]

**Abstract.** This paper presents a model which provides a smooth transition between a kinetic and a hydrodynamic domain. The idea is to use a buffer zone, in which both hydrodynamics and kinetic equations will be solved. The solution of the original kinetic equation will be recovered as the sum of the solutions of these two equations. We use an artificial connecting function which makes the equation on each domain degenerate at the end of the buffer zone, thus no boundary condition is needed at the transition point. Consequently this model avoids the delicate issue of finding the interface condition in a typical domain decomposition method that couples a kinetic equation with hydrodynamic equations. A simple kinetic scheme is developed to discretize our model, and numerical examples are used to validate the method.

**Key words.** Kinetic-Fluid coupling, Kinetic equation, Hydrodynamic approximation

**AMS subject classifications.** 82B40, 82B80, 82C40, 82C80, 76P05

# 1 Introduction

This work is devoted to a new method for the numerical simulation of kinetic models that involve different scales. These models allow for accurate descriptions of particles as in rarefied gases, neutron transport, or radiative transfer. However even with modern super-computers, the numerical solution of such models is still often impossible. Due to a very large number of degrees of freedom, they require too much computational time and memory space.

For some flow regimes, where the particles are in a near thermodynamical equilibrium state, there exist some simpler models that account for a correct physical description. These models are in some sense asymptotic approximations of the kinetic models, as the diffusion or the hydrodynamic limits. They are often called "fluid" or "macroscopic" models, in the sense that the microscopic behavior of the particles is neglected.

In fact, in many situations, the flow can be considered in equilibrium in the major part of the computational domain, except in some small zones where microscopic effects are important (as in shocks and close to the boundaries). In such cases, it is interesting to use the simpler macroscopic model wherever it is possible, and to restrict the use of the

[1]MIP, UMR 5640 (CNRS-UPS-INSA), Université Paul Sabatier, 118, Route de Narbonne, 31062 TOULOUSE cedex, France (degond@mip.ups-tlse.fr, mieussens@mip.ups-tlse.fr). Research supported by the European network HYKE, funded by the EU as contract no. HPRN-CT-2002-00282

[2]Department of Mathematics, University of Wisconsin, Madison, WI 53706, USA (jin@math.wisc.edu). Research supported by NSF grant No. DMS-0305080

kinetic model where it is necessary. This motivates a coupling method between kinetic and macroscopic models, already widely explored in neutron transport and radiative transfer (see for instance [4] and the references therein), where the macroscopic model is a linear diffusion limit. Here, we are instead interested in coupling kinetic equations with the hydrodynamic approximation. This approximation is for instance more relevant in, for example, rarefied gas dynamics for aerodynamical applications, where it can be either the Euler or Navier-Stokes equations.

We briefly give below a review of previous strategies in coupling the kinetic and hydrodynamic equations. One of the first methods (proposed by Coron in [2]) was to extend the validity of the hydrodynamic model near the boundaries by using boundary layer analysis. This method works well in linear transport with diffusion limit [20] but it becomes not efficient enough in the kinetic/hydrodynamic case.

During the past 15 years, several studies devoted to the coupling of Boltzmann model with Euler or Navier-Stokes equations for reentry problems in aerodynamics have been published. A first method was proposed by Bourgat, Le Tallec and Tidriri [1] who found new boundary conditions for the hydrodynamic equations by numerically solving the kinetic equation in the boundary layer ("coupling by friction"). Then Bourgat, Le Tallec, Malinger, and Qiu developed in [15, 17] a coupling by a domain decomposition approach. Similar methods were proposed by Neunzert, Struckmeier, Klar and Schneider [10, 16]. The common feature of these methods is that they are domain decomposition methods where the hydrodynamic and kinetic models are solved in different subdomains. The coupling relations are defined through suitable boundary conditions at the interface between the subdomains. These boundary conditions use continuity of moments or fluxes through the interface [10, 16], or a kinetic interpretation of the hydrodynamic fluxes [15, 17], or also boundary layer analyses [9, 8]. Mathematical analyses of these methods have also been proposed in [18] and [7].

Finally, a different and more recent method has been proposed by Tiwari [19] for which every cell of the computational domain can be considered to be in kinetic or hydrodynamic state, by using some physical criterion. This criterion determines whether the distribution function in the cell is evolved by some random collisional process or whether it is projected into the hydrodynamic equilibrium. However, this particle method is very expensive, since it uses as many degrees of freedom for the kinetic cells than for the hydrodynamic cells.

Recently, a new approach has been proposed by Degond and Jin [3] for the linear transport coupled with the diffusion approximation. Their idea is still to use a domain decomposition method, but in which the coupling is through the equations rather than the boundary conditions. This is done by using a buffer zone around the interface, and an artificial transition function that smoothly passes from 1 in the kinetic domain to 0 in the diffusion zone. The solution of the original transport equation is recovered as the sum of the solutions of the two models. This is different from the usual domain decomposition methods in which each of the models represents the full solution. The transition function makes the equation on each domain degenerate at the end of the buffer zone, thus no boundary condition is needed at this interface. This idea results in a very easy-to-use method that works very well in the linear case.

In this paper, we extend this approach to the nonlinear case, for coupling kinetic and hydrodynamic models. In particular, this applies to the coupling between the Boltzmann and Euler or Navier-Stokes equations. With this extension, we point out three new aspects

of the method:

- the equilibrium distribution must satisfy an homogeneity property such that the coupling method preserves uniform flows. This property was of course necessarily satisfied in [3] due to the linearity of the collision operator;
- we use a simple kinetic scheme to discretize our coupled model. Then we show that we recover the coupling method of [15, 17] when the buffer zone reduces to an interface;
- our method can be naturally adapted to the coupling with moving interface.

We now give the outline of the article. In section 2, we present a very general kinetic model, with a few important properties. Most of the usual kinetic models can be written in this form. Then we describe how to obtain a coupling of two kinetic models in two different subdomains by using a buffer zone and a transition function. From this model we deduce a coupling method between kinetic and hydrodynamic models and we study some of its properties in section 3. Two extensions of the method are proposed in section 4. The numerical method is given in section 5. In section 6, we present several numerical tests to illustrate the potential of our approach. Finally, a short conclusion is given in section 7.

# 2 The coupling method

## 2.1 Kinetic models and hydrodynamic limit

We present the method on a general kinetic equation in one space dimension. Let $f(t,x,v)$ represent the density of particles that at time $t$ have position $x \in (0,1)$ and velocity $v \in \mathbb{R}$ or any bounded or discrete subset of $\mathbb{R}$. The kinetic equation is

$$\partial_t f + v\partial_x f = Q(f). \tag{1}$$

The left hand-side of (1) describes the motion of the particles along the $x$ axis with velocity $v$, while the operator $Q$ takes into account the collisions between particles. This operator acts on $f$ only through the velocity locally at each $(t,x)$.

The integral of any scalar or vector valued function $f = f(v)$ over the velocity set is denoted by $\langle f \rangle = \int f(v)\, dv$.

The collision operator $Q$ is assumed to satisfy the local conservation property

$$\langle mQ(f) \rangle = 0 \qquad \text{for every } f,$$

where $m(v) = (m_i(v))_{i=1}^d$ are locally conserved quantities. Consequently, multiplying (1) by $m$ and integrating over the velocity set gives the local conservation laws

$$\partial_t \langle mf \rangle + \partial_x \langle vmf \rangle = 0. \tag{2}$$

Finally, we assume that the local equilibria of $Q$ (*i.e.* the solutions of $Q(f) = 0$) are equilibrium distributions $E[\rho]$, implicitly defined by their moments $\rho$ through the relation

$$\rho = \langle mE[\rho] \rangle.$$

We do not specify boundary conditions for the moment.

When the mean free path of the particles is very small compared with the size of the domain, *i.e.* when $Q$ is 'large', the numerical resolution of (1) can be very expensive, and it is worth using the asymptotic model obtained when $Q$ 'tends to infinity'. We introduce a new set of 'macroscopic variables' $x'$ and $t'$ according to

$$x' = \varepsilon x, \qquad t' = \varepsilon t,$$

where $\varepsilon$ denotes the ratio of the microscopic to the macroscopic scale. This parameter is often called the Knudsen number in rarefied gas dynamics. After using this change of variables and dropping the primes for simplicity, one gets

$$\partial_t f^\varepsilon + v\partial_x f^\varepsilon = \frac{1}{\varepsilon} Q(f^\varepsilon). \tag{3}$$

In the limit $\varepsilon \to 0$, $f^\varepsilon$ converges (at least formally) towards an equilibrium such that its moments are solutions of a system of hydrodynamic equations. More precisely, we have the formal result:

**Lemma 2.1.** *When $\varepsilon \to 0$, $f^\varepsilon$ converges to $E[\rho]$, where $\rho(t,x)$ is a solution of the system*

$$\partial_t \rho + \partial_x F(\rho) = 0, \tag{4}$$

*with initial condition $\rho|_{t=0} = \langle m f_0(x,v)\rangle$. The flux $F(\rho)$ is the equilibrium kinetic flux*

$$F(\rho) = \langle v m E[\rho]\rangle. \tag{5}$$

*Proof.* Formally, we just multiply (3) by $\varepsilon$, and let $\varepsilon$ go to 0. This gives $Q(f^{(0)}) = 0$ and thus $f^{(0)}$ is an equilibrium distribution $E[\rho]$. Since the conservation laws (2) are independent of $\varepsilon$, they are also satisfied in the limit $\varepsilon = 0$ by $f^{(0)}$. Since this function only depends on its moments $\rho$, this system is closed and leads to (4). □

## 2.2 The kinetic/kinetic coupling

The buffer interval is denoted by $[a,b]$. We introduce a smooth function $h(x)$ such that

$$\begin{cases} h(x) = 1, & \text{for} \quad x \le a, \\ h(x) = 0, & \text{for} \quad x \ge b, \\ h(x) \in [0,1] & \text{for} \quad a \le x \le b. \end{cases}$$

If we define the two distributions $f_L^\varepsilon = h f^\varepsilon$ and $f_R^\varepsilon = (1-h) f^\varepsilon$, then it is easy to check that they satisfy the following coupled system:

$$\partial_t f_L^\varepsilon + hv\partial_x f_L^\varepsilon + hv\partial_x f_R^\varepsilon = \frac{1}{\varepsilon} hQ(f_L^\varepsilon + f_R^\varepsilon), \tag{6}$$

$$\partial_t f_R^\varepsilon + (1-h)v\partial_x f_R^\varepsilon + (1-h)v\partial_x f_L^\varepsilon = \frac{1}{\varepsilon}(1-h)Q(f_L^\varepsilon + f_R^\varepsilon), \tag{7}$$

with initial data

$$f_L^\varepsilon|_{t=0} = h f_0, \qquad f_R^\varepsilon|_{t=0} = (1-h) f_0. \tag{8}$$

Indeed, we note the following:

**Lemma 2.2.** *If $(f_L^\varepsilon, f_R^\varepsilon)$ is the solution of problem (6-7) with initial data (8), then $f = f_L^\varepsilon + f_R^\varepsilon$ is the solution of problem (1) with inital condition $f_0$. Reciprocally, if $f$ is the solution of (1), then $(f_L^\varepsilon, f_R^\varepsilon) = (hf, (1-h)f)$ is the solution of (6-7) with the same initial condition.*

*Proof.* Just add up eqs. (6) and (7). For the converse statement, note that $\partial_t f_L^\varepsilon = h\partial_t f = -hv\partial_x f + \frac{1}{\varepsilon} hQ(f) = -hv\partial_x(f_L^\varepsilon + f_R^\varepsilon) + \frac{1}{\varepsilon} hQ(f_L^\varepsilon + f_R^\varepsilon)$ which gives (6). Eq. (7) is also obtained in this way. □

**Remark 2.1.** It could be attractive to put $h$ inside the $x$-derivative to obtain the following conservative coupling:

$$\partial_t f_L^\varepsilon + v\partial_x h f_L^\varepsilon + v\partial_x h f_R^\varepsilon = \frac{1}{\varepsilon} hQ(f_L^\varepsilon + f_R^\varepsilon), \tag{9}$$

$$\partial_t f_R^\varepsilon + v\partial_x[(1-h)f_R^\varepsilon] + v\partial_x[(1-h)f_L^\varepsilon] = \frac{1}{\varepsilon}(1-h)Q(f_L^\varepsilon + f_R^\varepsilon). \tag{10}$$

However, this coupling is not equivalent to the original kinetic equation (1), and moreover the corresponding kinetic/hydrodynamic coupling does not have good properties, see remark 3.1.

## 2.3 The kinetic/hydrodynamic coupling

Assume that $Q$ is of order $\varepsilon$ in the interval $(-\infty, a)$, and of order 1 in $(a, +\infty)$. In other words, we consider that the left region must be treated by a kinetic model while the right region can be approximated by the hydrodynamic equations. Therefore, we shall only be allowed to perform the hydrodynamic approximation on (7) while (6) will have to stay untouched. To this end, the source term of (7) is rewritten as $Q(f_L^\varepsilon + f_R^\varepsilon) = Q(f_R^\varepsilon) + [Q(f_L^\varepsilon + f_R^\varepsilon) - Q(f_R^\varepsilon)]$, and we assume that $Q(f_R^\varepsilon)$ is $O(1)$ whereas $[Q(f_L^\varepsilon + f_R^\varepsilon) - Q(f_R^\varepsilon)]$ is an $O(\varepsilon)$. Then (7) is rewritten as follows:

$$\begin{aligned} &\varepsilon\partial_t f_R^\varepsilon + \varepsilon(1-h)v\partial_x f_R^\varepsilon - (1-h)Q(f_R^\varepsilon) \\ &\qquad = -\varepsilon(1-h)v\partial_x f_L^\varepsilon + (1-h)[Q(f_L^\varepsilon + f_R^\varepsilon) - Q(f_R^\varepsilon)] \end{aligned} \tag{11}$$

where the right-hand-side is considered to be $O(\varepsilon)$.

The following proposition states what the hydrodynamic approximation $\varepsilon \to 0$ of this equation is.

**Proposition 2.1.** *Consider Eq. (11) where the right-hand-side is treated as an $O(\varepsilon)$ term. Then as $\varepsilon \to 0$, $f_R^\varepsilon \approx$ equilibrium $E[\rho_R^\varepsilon]$, where $\rho_R^\varepsilon(t,x)$ is a solution of the following hydrodynamic system:*

$$\partial_t \rho_R^\varepsilon + (1-h)F(\rho_R^\varepsilon) + (1-h)\langle vmf_L^\varepsilon\rangle = 0, \tag{12}$$

*with $F(\rho_R^\varepsilon)$ defined by (5).*

As noted in [3], since $\varepsilon$ tends to 0 only in some terms and not in others, we cannot speak of convergence, but rather, of asymptotic equivalence, hence the use of the symbol $\approx$.

Note that (12) is a hydrodynamic equation in $(a, +\infty)$. However no boundary condition is needed in $x = a$, since the flux is cancelled by $1 - h$.

*Proof.* We first note that taking the moments of (7) gives

$$\partial_t \rho_R^\varepsilon + (1-h)\partial_x \langle vm f_R^\varepsilon \rangle + (1-h)\partial_x \langle vm f_L^\varepsilon \rangle = 0. \tag{13}$$

Now as in Lemma 2.1, we let $\varepsilon$ go to 0 in (11) to find $Q(f_R^0) = 0$, hence $f_R^0 = E[\rho_R^0]$. Then (12) is obtained as the limit $\varepsilon = 0$ of (13). However, $\rho_R^0$ still depends on $\varepsilon$ through $f_L^\varepsilon$: this is why it is denoted by $\rho_R^\varepsilon$ in the proposition. □

Now, the coupled kinetic/hydrodynamic model is written as follows:

$$\partial_t f_L^\varepsilon + hv\partial_x f_L^\varepsilon + hv\partial_x E[\rho_R^\varepsilon] = \frac{1}{\varepsilon} hQ(f_L + E[\rho_R^\varepsilon]), \tag{14}$$

$$\partial_t \rho_R^\varepsilon + (1-h)\partial_x F(\rho_R^\varepsilon) + (1-h)\partial_x \langle vm f_L^\varepsilon \rangle = 0, \tag{15}$$

with initial data

$$f_L^\varepsilon|_{t=0} = hf_0, \quad \rho_R^\varepsilon|_{t=0} = (1-h)\rho_0. \tag{16}$$

Therefore, this coupled model will be used to approximate by $f_L^\varepsilon + E[\rho_R^\varepsilon]$ the solution $f^\varepsilon$ of model (3). More precisely, $f^\varepsilon$ is supposed to be approximated by $f_L^\varepsilon$ in $(0, a)$, by $f_L^\varepsilon + E[\rho_R^\varepsilon]$ in $(a, b)$, and by $E[\rho_R^\varepsilon]$ in $(b, 1)$.

To simplify the notations in the remainder of the paper, the superscript $\varepsilon$ will be omitted when no confusion is caused.

# 3 Properties of the kinetic/hydrodynamic coupling

## 3.1 Preservation of uniform flows

Uniform flows for model (1) are constant equilibrium distributions $f = E[\rho]$. Because of the function $h$, $f$ is approximated in the coupled model (14-16) by non-uniform distributions. Then it is not clear whether the approximation $f_L + E[\rho_R]$ given by the coupled model (14-16) is still a uniform distribution. However, this preservation property is desirable to prevent oscillations in zones where the flow should be uniform (a similar phenomenon is known in computational fluid dynamics when one wants to discretize conservation laws written in curvilinear coordinates, see [22]). As it is shown in the following proposition, the preservation of uniform flows is related to a particular property of the equilibrium.

**Proposition 3.1.** *Assume the mapping $\rho \mapsto E[\rho]$ is homogeneous of degree 1, that is*

$$E[\lambda\rho] = \lambda E[\rho] \tag{17}$$

*for every $\lambda \geq 0$ and every $\rho$ in the definition domain of $E$. If the initial condition $f^0$ is a constant equilibrium $E[\rho]$, then $f_L = hE[\rho]$ and $\rho_R = (1-h)\rho$ are solutions of the coupled model (14-16), and $f_L + E[\rho_R] = E[\rho]$.*

*Proof.* First, note that the homogeneity property implies $E[\rho_R] = E[(1-h)\rho] = (1-h)E[\rho]$. Therefore it is clear that $f_L + E[\rho_R] = E[\rho]$. Moreover, putting the collision operator in the

left-hand-side of (14) and using again the homogeneity of $E$, we find that this left-hand-side is

$$\begin{aligned}
&\partial_t f_L + hv\partial_x f_L + hv\partial_x E[\rho_R] - \frac{1}{\varepsilon} hQ(f_L + E[\rho_R]) \\
&= \partial_t hE[\rho] + hv\partial_x(hE[\rho]) + hv\partial_x E[(1-h)\rho] - \frac{1}{\varepsilon} hQ(E[\rho]) \\
&= 0 + hvh'E[\rho] - hvh'E[\rho] - 0 = 0,
\end{aligned}$$

thus $(f_L, \rho_R)$ solves (14).

Then note that the equilibrium flux $F$ defined by (5) inherits the homogeneity property of $E$, and therefore the left-hand-side of (15) reads

$$\begin{aligned}
&\partial_t \rho_R + (1-h)\partial_x F(\rho_R) + (1-h)\partial_x \langle vm f_L \rangle \\
&= \partial_t (1-h)\rho + (1-h)\partial_x F((1-h)\rho) + (1-h)\partial_x \langle vmhE[\rho] \rangle \\
&= 0 - (1-h)h'\partial_x F(\rho) + (1-h)h'\langle vmE[\rho] \rangle = 0,
\end{aligned}$$

thus $(f_L, \rho_R)$ solves (15). □

As it is shown in the following examples, a large class of models satisfy assumption (17), even if some other models do not.

**Example 3.1.** Classical models of kinetic theory for rarefied gases and plasmas (Boltzmann, BGK, Fokker-Planck-Landau) satisfy property (17). These models use Maxwell-Boltzmann statistics for which the equilibrium is the Maxwellian distribution defined by

$$E[\rho] = \frac{n}{(2\pi\theta)^{1/2}} \exp\Big(-\frac{(v-u)^2}{2\theta}\Big).$$

The moment vector of this equilibrium is $\rho = (n, nu, \frac{1}{2}nu^2 + \frac{1}{2}n\theta)$. This shows that the velocity $u = \frac{\rho_2}{\rho_1}$ and temperature $\theta = \frac{2}{\rho_1}(\rho_3 - \frac{\rho_2^2}{\rho_1})$ are homogeneous functions of degree 0 of $\rho$, whereas the density $n = \rho_1$ is homogeneous of degree 1. Consequently, $E$ is clearly homogeneous of degree 1.

**Example 3.2.** Kinetic models derived with Fermi-Dirac or Bose-Einstein statistics do not satisfy constraint (17). In that case the equilibrium is given by

$$E[\rho] = \frac{1}{\exp(\frac{\epsilon-\mu}{\tau}) \pm 1} \qquad (+ \text{ Fermi-Dirac, - Bose-Einstein}).$$

In the Fermi-Dirac case, it is bounded by 1 and thus cannot be homogeneous of degree 1.

**Example 3.3.** A simpler model that does not satisfy this constraint (17) is the following discrete kinetic equation

$$\partial_t u + \partial_x u = \frac{1}{\tau}(M_1[\rho] - u), \qquad \partial_t v - \partial_x v = \frac{1}{\tau}(M_2[\rho] - v), \tag{18}$$

where the equilibrium is $(M_1[\rho], M_2[\rho]) = \frac{1}{2}(\rho + f(\rho), \rho - f(\rho))$, with $f(\rho) = \frac{1}{2}\rho^2$ and $\rho = u + v$.

This model has the same form as (1) with discrete velocities $v = \pm 1$ and collisional invariants $m(v) = 1$. It is equivalent to the Jin-Xin relaxation model

$$\partial_t \rho + \partial_x j = 0, \qquad \partial_t j + \partial_x \rho = \frac{1}{\tau}(f(\rho) - j),$$

with $j = u - v$. It can be shown to relax towards the conservation law $\partial_t \rho + \partial_x f(\rho) = 0$ as $\tau \to 0$ [6].

Clearly, the equilibrium is not a homogeneous function of $\rho$. In that case, simple calculations show that conclusions of proposition (3.1) are false. As a consequence, the coupled model derived from this system behaves incorrectly in zones where the solution should be uniform.This will be shown in section 6.

**Remark 3.1.** The kinetic/hydrodynamic coupling for the conservative coupling (9-10) is

$$\partial_t f_L^\varepsilon + v\partial_x h f_L^\varepsilon + v\partial_x h E[\rho_R^\varepsilon] = \frac{1}{\varepsilon} h Q(f_L + E[\rho_R^\varepsilon]),$$
$$\partial_t \rho_R^\varepsilon + \partial_x[(1-h)F(\rho_R^\varepsilon)] + \partial_x[(1-h)\langle v m f_L^\varepsilon\rangle] = 0.$$

Although this conservative form seems better for numerics, it can be seen (with the same analysis as in the proof of proposition 3.1) that this system does not preserve uniform flows.

## 3.2 Full hydrodynamic limit

Here we prove that if both regions are hydrodynamic, we recover the global hydrodynamic equation (4) for $\rho = \rho_L + \rho_R$.

**Proposition 3.2.** *As $\varepsilon \to 0$, the moments $(\rho_L^\varepsilon, \rho_R^\varepsilon)$ of the solution of the coupled model (14-15) converge to $(\rho_L, \rho_R)$, a solution of the hydrodynamic system*

$$\partial_t \rho_L + h\partial_x F(\rho_L + \rho_R) = 0, \tag{19}$$
$$\partial_t \rho_R + (1-h)\partial_x F(\rho_L + \rho_R) = 0, \tag{20}$$

*with initial data*

$$\rho_L|_{t=0} = h\rho_0, \quad \rho_R|_{t=0} = (1-h)\rho_0. \tag{21}$$

*In particular, $\rho = \rho_L + \rho_R$ is a solution of (4).*

*Proof.* The proof is similar to that of proposition 2.1. First, we take the moments of (14) to obtain

$$\partial_t \rho_L^\varepsilon + h\partial_x \langle v m f_L^\varepsilon\rangle + h\partial_x F(\rho_R^\varepsilon) = 0. \tag{22}$$

Then multiplying (14) by $\varepsilon$ and taking the limit $\varepsilon = 0$ gives $Q(f_L^0 + E[\rho_R^0]) = 0$. Therefore $f_L^0 + E[\rho_R^0] = E[\rho]$, where we necessarily have $\rho = \rho_L^0 + \rho_R^0$. Consequently

$$f_L^0 = E[\rho_L^0 + \rho_R^0] - E[\rho_R^0]. \tag{23}$$

Now we take the limit $\varepsilon = 0$ in (22), and use (23) to find

$$\partial_t \rho_L^0 + h\partial_x F(\rho_L^0 + \rho_R^0) = 0,$$

which is nothing but (19) where the superscript 0 is dropped. Then by taking the limit $\varepsilon = 0$ of (15) and using again (23) yields

$$\partial_t \rho_R^0 + (1-h)\partial_x F(\rho_L^0 + \rho_R^0) = 0,$$

which is (20) after the superscript 0 is dropped.

Finally, if one adds up (19) and (20), it is clear that $\rho = \rho_L + \rho_R$ satisfies (4).

□

### 3.3 Limit $b - a = 0$ of the coupling method

As recalled in the introduction, some previous coupling methodologies use a coupling by an interface. Therefore it is interesting to know if we can recover some of these models by taking the limit $b - a = 0$ in our coupling model (14-15).

However, in this limit, $h$ tends to the Heaviside function, and it looks difficult to know what the limit of fluxes as $h(x)\partial_x f_L$ is.

See section 5.2 for such a study at the discrete level.

## 4 Extensions of the coupling method

### 4.1 Second order coupling method : kinetic/Navier-Stokes

First, in the kinetic/kinetic coupling (6-7), we take the moments of the second equation to obtain the following (non-closed) system

$$\partial_t f_L^\varepsilon + hv\partial_x f_L^\varepsilon + hv\partial_x f_R^\varepsilon = \frac{1}{\varepsilon} hQ(f_L^\varepsilon + f_R^\varepsilon), \tag{24}$$

$$\partial_t \rho_R^\varepsilon + (1-h)\partial_x \langle vm f_R^\varepsilon \rangle + (1-h)\partial_x \langle vm f_L^\varepsilon \rangle = 0. \tag{25}$$

By expanding $f_R^\varepsilon$ as $f_R^\varepsilon = E[\rho_R^\varepsilon] + \varepsilon f_R^1$, one defines $f_R^1$ and implies that its moments are zero, namely $\langle m f_R^1 \rangle = 0$. Write the flux of $f_R^\varepsilon$ as

$$\langle vm f_R^\varepsilon \rangle = F(\rho_R^\varepsilon) + q,$$

where $q$ is defined by

$$q = \varepsilon \langle vm f_R^1 \rangle. \tag{26}$$

Therefore, the non closed system (24-25) can now be written as

$$\partial_t f_L^\varepsilon + hv\partial_x f_L^\varepsilon + hv\partial_x f_R^\varepsilon = \frac{1}{\varepsilon} hQ(f_L^\varepsilon + f_R^\varepsilon), \tag{27}$$

$$\partial_t \rho_R^\varepsilon + (1-h)\partial_x F(\rho_R^\varepsilon) + (1-h)\partial_x \langle vm f_L^\varepsilon \rangle = -(1-h)\partial_x q. \tag{28}$$

Since from (26) $q$ is $O(\varepsilon)$, it is clear that this system reduces to the first order kinetic/hydrodynamic system (14-15) as $\varepsilon = 0$. Now, to obtain a second order closure, one has to approximate $q$ up to the first order. This is done by determining the perturbation $f_R^1$

up to $O(\varepsilon)$. To do so, insert the expansion of $f_R^\varepsilon$ in (7) and make the same assumptions as in proposition 2.1 about the size of $Q$. Then, at first order in $\varepsilon$, one finds that $f_R^1$ satisfies

$$\begin{aligned}(1-h)DQ(E[\rho_R^\varepsilon])f_R^1 \\ = \partial_t E[\rho_R^\varepsilon] + (1-h)v\partial_x E[\rho_R^\varepsilon] + (1-h)v\partial_x f_L^\varepsilon - (1-h)\Delta,\end{aligned} \tag{29}$$

where $\Delta = \frac{1}{\varepsilon}[Q(f_L^\varepsilon + f_R^\varepsilon) - Q(f_R^\varepsilon)]$ is supposed to be $O(1)$, and $DQ(f)$ is the derivative of $Q$ with respect to $f$.

In order to have simpler calculations, we assume that $Q$ is the following BGK operator

$$Q(f) = \frac{1}{\tau(\rho)}(E[\rho] - f), \tag{30}$$

where $\rho = \langle mf\rangle = (n, nu, \frac{1}{2}nu^2 + \frac{1}{2}n\theta)$, with collisional invariants defined by $m(v) = (1, v, \frac{1}{2}|v|^2)$. The variables $u$ and $\theta$ are called the velocity and temperature associated to $f$.

Since the moments of $f_R^1$ are zero, it can easily be proved that $DQ(E[\rho_R^\varepsilon])f_R^1 = -\frac{1}{\tau(\rho_R^\varepsilon)}f_R^1$. Consequently $f_R^1$ can be explicitly computed:

$$f_R^1 = -\tau(\rho_R^\varepsilon)\left(\frac{1}{1-h}\partial_t E[\rho_R^\varepsilon] + \partial_x E[\rho_R^\varepsilon] + \partial_x f_L^\varepsilon + \Delta\right). \tag{31}$$

Moreover, since the collisional invariants are $m(v) = (1, v, \frac{1}{2}|v|^2)$ for BGK, one has

$$q = \begin{pmatrix} 0 \\ 0 \\ \varepsilon\langle\frac{1}{2}(v-u_R)^3 f_R^1\rangle \end{pmatrix}, \tag{32}$$

where $u_R$ is the velocity associated to $f_R^\varepsilon$. Note that since our problem is in one dimension in space, there is no shear-stress in $q$ (its second component is zero). Consequently, if $f_R^1$ is inserted in the third component $q_3$ of $q$, one obtains

$$\begin{aligned}q_3 = -\varepsilon\tau(\rho_R^\varepsilon)\Big(\frac{1}{1-h}\langle\tfrac{1}{2}(v-u_R)^3\partial_t E[\rho_R^\varepsilon]\rangle + \langle\tfrac{1}{2}(v-u_R)^3 v\partial_x E[\rho_R^\varepsilon]\rangle + \langle\tfrac{1}{2}(v-u_R)^3 v\partial_x f_L^\varepsilon\rangle \\ + \langle\tfrac{1}{2}(v-u_R)^3\Delta\rangle\Big).\end{aligned}$$

After classical but tedious computations (in which the first order approximation of (28) is used to remove the time derivative), one finds

$$\begin{aligned}q_3 = &-\varepsilon\frac{3}{2}\tau(\rho_R^\varepsilon)n_R\theta_R\partial_x\theta_R \\ &-\varepsilon\tau(\rho_R^\varepsilon)\langle[-\frac{3}{2}\theta_R + \tfrac{1}{2}(v-u_R)^2](v-u_R)v\partial_x f_L^\varepsilon\rangle \\ &+\varepsilon\tau(\rho_R^\varepsilon)\langle\tfrac{1}{2}(v-u_R)^3\Delta\rangle,\end{aligned}$$

where $n_R, u_R, \theta_R$ are respectively the density, velocity and temperature associated to $f_R^\varepsilon$.

The first term is the heat-flux $\kappa\partial_x\theta_R$ of the Fourier law, where the thermal conductivity is $\kappa = \frac{3}{2}\varepsilon\tau(\rho_R^\varepsilon)n_R\theta_R$. This term is only due to $f_R^\varepsilon$. In the second line, the coupling between the $f_R^\varepsilon$ and $f_L^\varepsilon$ has no obvious interpretation.

Note that in the third line of the last expression, $\Delta = \frac{1}{\varepsilon}[Q(f_L^\varepsilon + f_R^\varepsilon) - Q(f_R^\varepsilon)]$ has not yet been expanded. To do so, we have to make a new assumption on $f_L^\varepsilon$: we shall assume that $f_L^\varepsilon$ is $O(\varepsilon)$. This is a reasonable choice near $x = b$ of the buffer zone, but is yet difficult to justify near $x = a$. For the moment, we will neglect this problem to derive the model; the numerical tests of the model will a posteriori justify (or not) this assumption. Therefore $\Delta$ can be expanded as

$$\Delta = \frac{1}{\varepsilon}DQ(E[\rho_R^\varepsilon])(f_L^\varepsilon)$$

with an $O(\varepsilon)$ error.

Finally, we resume below the final second order kinetic/Navier-Stokes coupling, obtained with the BGK collision operator (30):

$$\partial_t f_L^\varepsilon + hv\partial_x f_L^\varepsilon + hv\partial_x f_R^\varepsilon = \frac{1}{\varepsilon}hQ(f_L^\varepsilon + f_R^\varepsilon), \tag{33}$$

$$\partial_t \rho_R^\varepsilon + (1-h)\partial_x F(\rho_R^\varepsilon) + (1-h)\partial_x\langle vmf_L^\varepsilon\rangle = -(1-h)\partial_x q, \tag{34}$$

where $f_R^\varepsilon$ can be approximated by $E[\rho_R^\varepsilon]$ or by $E[\rho_R^\varepsilon] + \varepsilon f_R^1$. Moreover, we have $q = (0, 0, q_3)^T$ with

$$\begin{aligned} q_3 = &-\varepsilon\frac{3}{2}\tau(\rho_R^\varepsilon)n_R\theta_R\partial_x\theta_R \\ &-\varepsilon\tau(\rho_R^\varepsilon)\langle[-\frac{3}{2}\theta_R + \tfrac{1}{2}(v-u_R)^2](v-u_R)v\partial_x f_L^\varepsilon\rangle \\ &+\varepsilon\tau(\rho_R^\varepsilon)\langle\tfrac{1}{2}(v-u_R)^3\Delta\rangle, \end{aligned} \tag{35}$$

and

$$\Delta = \frac{1}{\varepsilon}DQ(E[\rho_R^\varepsilon])(f_L^\varepsilon). \tag{36}$$

Finally, $n_R$, $u_R$ and $\theta_R$ are defined by $\rho_R^\varepsilon$ through the relation $\rho_R^\varepsilon = (n_R, n_R u_R, \frac{1}{2}n_R u_R^2 + \frac{1}{2}n_R\theta_R)$.

The numerical study of this model will not be done in this paper and is deferred to a future work.

## 4.2 Moving buffer zone

In this section, we show that our models can be extended to the case where $h$ is time dependent. In that case, the method can be extended to moving interface regions: $h$ can actually be defined as a level set function, and can evolve according to its own dynamics, such as a Hamilton-Jacobi equation for front propagation, or other kinds of dynamics.

If we simply let $h$ depend on time in the coupled model (14-15), it turns out that it is no longer uniform-flow preserving. The correct way to proceed is to derive a kinetic/kinetic model as we did in the beginning of section 2.2. First, if $f^\varepsilon$ is the solution of the kinetic

equation (1), we set $f_L^\varepsilon = hf^\varepsilon$ and $f_R^\varepsilon = (1-h)f^\varepsilon$. Then one can easily derive the following equations satisfied by $f_L^\varepsilon$ and $f_R^\varepsilon$

$$\partial_t f_L^\varepsilon + hv\partial_x f_L^\varepsilon + hv\partial_x f_R^\varepsilon = \frac{1}{\varepsilon} hQ(f_L^\varepsilon + f_R^\varepsilon) + (f_L^\varepsilon + f_R^\varepsilon)\partial_t h,$$
$$\partial_t f_R^\varepsilon + (1-h)v\partial_x f_R^\varepsilon + (1-h)v\partial_x f_L^\varepsilon = \frac{1}{\varepsilon}(1-h)Q(f_L^\varepsilon + f_R^\varepsilon) - (f_L^\varepsilon + f_R^\varepsilon)\partial_t h.$$

This system is equivalent to the kinetic equation (1), and the corresponding kinetic/hydrodynamic model is found to be

$$\partial_t f_L^\varepsilon + hv\partial_x f_L^\varepsilon + hv\partial_x E[\rho_R^\varepsilon] = \frac{1}{\varepsilon} hQ(f_L + E[\rho_R^\varepsilon]) + (f_L^\varepsilon + E[\rho_R^\varepsilon])\partial_t h,$$
$$\partial_t \rho_R^\varepsilon + (1-h)\partial_x F(\rho_R^\varepsilon) + (1-h)\partial_x \langle vmf_L^\varepsilon\rangle = -(\rho_L^\varepsilon + \rho_R^\varepsilon)\partial_t h.$$

Owing to the new forcing term involving $\partial_t h$, a simple extension of the proof of proposition 3.1 shows that this system now preserves uniform flows.

The numerical investigation of this model is deferred to a future work.

# 5 Numerical schemes

## 5.1 A simple kinetic scheme

First, we present a simple spatial discretization for which the time and velocity variables are kept continuous. The space variable $x$ is discretized with mesh points $x_i = i\Delta x$ for $i = 1, \dots, i_{max}$ and we define $i_a$ and $i_b$ such that $x_{i_a} = a$ and $x_{i_b} = b$. We set $h_i = h(x_i)$, $f_{L,i} = f_L(x_i)$, and $\rho_{R,i} = \rho_R(x_i)$. Note that for more clarity, the $\varepsilon$ is dropped in this section.

This discretization uses the kinetic scheme (see for instance [14]). It consists of two main steps: (1) discretization of the kinetic/kinetic coupling (6-7), (2) projection of $f_R$ to the equilibrium $E[\rho_R]$ in the discretized system. These steps are detailed below.

**Discretization of the kinetic/kinetic coupling (6-7):**

The system (6-7) can be written as

$$\partial_t U + A\partial_x U = S, \tag{37}$$

where $U = \begin{pmatrix} f_L \\ f_R \end{pmatrix}$, $A = v\begin{pmatrix} h & h \\ 1-h & 1-h \end{pmatrix}$ and $S = \begin{pmatrix} hQ(f_L+f_R) \\ (1-h)Q(f_L+f_R) \end{pmatrix}$. The eigenvalues of $A$ are 0 and $v$, therefore for each $v$ this system is a linear hyperbolic system with source term. This system is discretized below by following the classical procedure: (a) diagonalization, (b) upwind discretization, (c) back to the original variables (see for instance [11]).

*(a) diagonalization*

The matrix of eigenvectors of $A$ is $P = \begin{pmatrix} 1 & 1 \\ -1 & \frac{1-h}{h} \end{pmatrix}$. Multiplying (37) by $P^{-1}$ and defining the characteristic variables $V = \begin{pmatrix} \alpha \\ \beta \end{pmatrix} = P^{-1}U$, we get the following diagonalized system

$$\partial_t V + D\partial_x V = T,$$

where $D = \left(\begin{smallmatrix} 0 & 0 \\ 0 & v \end{smallmatrix}\right) = P^{-1}AP$ and $T = P^{-1}S$. The two components of this system are

$$\begin{aligned} &\partial_t \alpha = T_1 \\ &\partial_t \beta + v\partial_x \beta = T_2. \end{aligned}$$

*(b) Upwind discretization*

The system can be discretized by upwinding the space derivative $\partial_x \beta$ following the sign of $v$ :

$$\begin{aligned} &\partial_t \alpha_i = (T_1)_i \\ &\partial_t \beta_i + v^+ \frac{\beta_i - \beta_{i-1}}{\Delta x} + v^- \frac{\beta_{i+1} - \beta_i}{\Delta x} = (T_2)_i, \end{aligned} \tag{38}$$

where $\beta_i$ stands fo $\beta(x_i)$ and $v^\pm = \frac{1}{2}(v \pm |v|)$ is the positive/negative part of $v$.

*(c) Back to the original variables*

The semi-discrete system (38) can be written as

$$\partial_t V_i + D^+ \frac{V_i - V_{i-1}}{\Delta x} + D^- \frac{V_{i+1} - V_i}{\Delta x} = T_i,$$

where we set $D^\pm = \left(\begin{smallmatrix} 0 & 0 \\ 0 & v^\pm \end{smallmatrix}\right)$. By going back to the original variables $U = PV$ after multiplying this system by $P$, one gets

$$\partial_t U_i + A_i^+ \frac{U_i - U_{i-1}}{\Delta x} + A_i^- \frac{U_{i+1} - U_i}{\Delta x} = S_i,$$

where $A_i^\pm = P_i D^\pm P_i^{-1} = v^\pm \left(\begin{smallmatrix} h_i & h_i \\ 1-h_i & 1-h_i \end{smallmatrix}\right)$. We can write this system componentwise: this gives the following discretization of the kinetic/kinetic coupling (6-7)

$$\begin{aligned} &\partial_t f_{L,i} + h_i \frac{\phi_{i+\frac{1}{2}}(f_L) - \phi_{i-\frac{1}{2}}(f_L)}{\Delta x} + h_i \frac{\phi_{i+\frac{1}{2}}(f_R) - \phi_{i-\frac{1}{2}}(f_R)}{\Delta x} \\ &\quad = h_i Q(f_{L,i} + f_{R,i}), \end{aligned} \tag{39}$$

$$\begin{aligned} &\partial_t f_{R,i} + (1-h_i) \frac{\phi_{i+\frac{1}{2}}(f_R) - \phi_{i-\frac{1}{2}}(f_R)}{\Delta x} + (1-h_i) \frac{\phi_{i+\frac{1}{2}}(f_L) - \phi_{i-\frac{1}{2}}(f_L)}{\Delta x} \\ &\quad = (1-h_i) Q(f_{L,i} + f_{R,i}), \end{aligned} \tag{40}$$

where the numerical flux

$$\phi_{i+\frac{1}{2}}(g) = v^- g_{i+1} + v^+ g_i, \tag{41}$$

for every $i$.

Note that this semi-discrete scheme could in fact be directly derived from system (6-7) without using the diagonalization step. This is a general property of $2 \times 2$ linear hyperbolic systems $\partial_t U + A\partial_x U = 0$ with matrix $A = \left(\begin{smallmatrix} a & a \\ b & b \end{smallmatrix}\right)$ such that $ab > 0$. Indeed, a direct upwind discretization of this system following the sign of the elements of $A$ gives the semi-discrete

scheme $\partial_t U_i + A^+ \frac{U_i - U_{i-1}}{\Delta x} + A^- \frac{U_{i+1} - U_i}{\Delta x} = 0$, while it can easily be proved that the previous procedure (diagonalization, discretization, back to original variables) always leads to the same scheme.

**Projection of $f_R$ to the equilibrium $E[\rho_R]$:**

Now $f_R$ is replaced by the equilibrium $E[\rho_R]$ in (39-40) and we take the moments of (40) to obtain the following scheme for the coupling (14-15)

$$\begin{aligned}
&\partial_t f_{L,i} + h_i \frac{\phi_{i+\frac{1}{2}}(f_L) - \phi_{i-\frac{1}{2}}(f_L)}{\Delta x} + h_i \frac{\phi_{i+\frac{1}{2}}(E[\rho_R]) - \phi_{i-\frac{1}{2}}(E[\rho_R])}{\Delta x} \\
&\quad = h_i Q(f_{L,i} + E[\rho_{R,i}]), \qquad (42) \\
&\partial_t \rho_{R,i} + (1-h_i) \frac{F_{i+\frac{1}{2}}(\rho_R) - F_{i-\frac{1}{2}}(\rho_R)}{\Delta x} + (1-h_i) \frac{\langle m(\phi_{i+\frac{1}{2}}(f_L) - \phi_{i-\frac{1}{2}}(f_L))\rangle}{\Delta x} \\
&\quad = 0, \qquad (43)
\end{aligned}$$

where

$$F_{i+\frac{1}{2}}(\rho_R) = \langle m \phi_{i+\frac{1}{2}}(E[\rho_R])\rangle$$

is a consistent approximation of $F(\rho_R)$.

Note that $f_{L,i} = 0$ for $i \geq i_b$ and $\rho_{R,i} = 0$ for $i \leq i_a$, since the fluxes are cancelled by $h$ and $1-h$ in these zones.

Moreover, it is clear that this scheme preserves uniform flows (the same proof as that of proposition 3.1 can be made).

In our numerical tests, the time variable is discretized by using a simple explicit Euler method. However, very small time step restrictions can occur due to the kinetic part of the model. Then a time stepping algorithm is used to advance differently the hyperbolic and kinetic parts when necessary. If the time step $\Delta t_K$ imposed by the kinetic part is much lower than the time step $\Delta t_H$ due to the hydrodynamic part, we solve the kinetic equation (42) during $N = [\Delta t_H / \Delta t_K]$ time steps $\Delta t_K$ with a constant hydrodynamic contribution. Then the hydrodynamic equation (43) is solved with time step $\Delta t_H$.

Finally, integrals in the velocity variable are discretized by the rectangle formula.

## 5.2 Limit $b - a = 0$

In this section, we prove that when $b - a \to 0$, the scheme given in section 5.1 gives a scheme close to that proposed in [15] for coupling Boltzmann/Euler by an interface half-flux condition.

The limit $b - a = 0$ can be considered by replacing $h$ in scheme (42-43) by $h^\delta(x) := h(\frac{b-a}{\delta}(x-a) + a)$. Indeed as $\delta \to 0$, $h^\delta$ tends to the Heaviside function $H(x-a)$, and the buffer zone $[a, a+\delta]$ tends to the interface $x = a$.

When $\delta < \Delta x$ then $h_i^\delta = 1$ for $i \leq i_a$ and 0 for $i \geq i_a + 1$. Consequently, the coupling terms in (42-43) vanish, except $v^- E[\rho_{R,i_a+1}]$ in (42) for $i = i_a$ and $\langle m v^+ f_{L,ia}\rangle$ in (43) for $i = i_a + 1$. Then a simple calculation shows that (42-43) gives in the limit $\delta = 0$ the following

scheme

$$\partial_t f_{L,i} + \frac{\phi_{i+\frac{1}{2}}(f_L) - \phi_{i-\frac{1}{2}}(f_L)}{\Delta x} = h_i Q(f_{L,i}), \qquad i \le i_a,$$
$$\partial_t \rho_{R,i} + \frac{\langle m(\phi_{i+\frac{1}{2}}(E[\rho_R]) - \phi_{i-\frac{1}{2}}(E[\rho_R]))\rangle}{\Delta x} = 0, \qquad i \ge i_a + 1,$$

with "interface half-flux condition"

$$v^- f_{L,i_a+1} = v^- E[\rho_{R,i_a+1}],$$
$$\langle v^+ m E[\rho_{R,i_a}]\rangle = \langle v^+ m f_{L,i_a}\rangle.$$

This scheme is close to the coupling method proposed in [15], and developed in [17]. Indeed, this can be viewed as an upwind scheme with kinetic flux vector splitting for the coupled model

$$\partial_t f + v\partial_x f = Q(f), \qquad 0 \le x \le a,$$
$$\partial_t \rho + \partial_x F(\rho) = 0, \qquad a \le x \le 1,$$

with interface half-flux condition

$$v^- f|_{x=a} = v^- E[\rho]|_{x=a},$$
$$\langle v^+ m E[\rho]\rangle|_{x=a} = \langle v^+ m f\rangle|_{x=a}.$$

In that sense, our method can be viewed as a justification (as well as an extension) of this method.

Moreover, in higher dimension, when the interface is complicated, the method of [15, 17] needs the implementation of the interface flux condition in a complicated way, while our method based on the introduction of a smoothing function $h$ transfers the geometry to the PDE. This is an advantage, since it is then possible to solve the PDE in a regular geometry while completely ignoring the real interface geometry. One just has to choose $h$ first according to the interface geometry initially, then forget about the geometry and solves the PDE on regular grids.

# 6 Numerical results

In this section, we first present several numerical solutions of the coupling model (14-15) corresponding to two kinetic models that can be written in form (1). These models are considered in the domain $[0, 1]$ with Neumann boundary conditions

$$\partial_x f(t, 0, v^+) = 0 \qquad \text{and} \qquad \partial_x f(t, 1, v^-) = 0,$$

and an initial data in equilibrium state $f(0, x, v) = E[\rho(x)]$.

For 1D problems, there are not to many different tests that can be made. Here, we mainly study the propagation of shocks, which is typical of aerodynamical flows. In this case, it can be assumed that the flow is close to equilibrium far from the shock, and in a non-equilibrium

regime near the shock. Then it seems natural to use our coupling model with kinetic and hydrodynamic zones located near and far from the shock, respectively. Traditionally in these classical shock problems, the shock is considered to move from left to right: this makes it necessary to reverse the order used in model (14-15) for our different zones. In other words, we shall consider that the left region is in equilibrium and can be treated by a hydrodynamic model, while the right region must be treated by a kinetic equation. For simplicity, we shall take a hydrodynamic zone on the left side, a buffer zone around the initial position of the shock, and a kinetic zone on the right side.

We shall successively consider the Jin-Xin relaxation approximation (18) of the Burgers equation and a BGK model similar to (30) that is 1D in space but 3D in velocity. In the first case, we shall experimentally demonstrate that the coupling method does not preserve uniform flows, as was noticed in example 3.3. In the second case, we shall see that the coupling method behaves satisfactorily.

We shall also present a test for the BGK model in two space dimensions. As explained in section 5.2, this test shows our method also applies to 2D flows and behaves well.

**Example 6.1.** Numerical solution of the coupling method for the Jin-Xin relaxation approximation (18) of the Burgers equation.

Here we take $\varepsilon = 0.01$. We use 100 points to solve the kinetic model (18) in the entire domain, and 100 points for the numerical approximation of the coupling model. The function $h$ is defined to be piecewise linear and continuous: 0 for $x \leq a$, 1 for $x \geq b$, and linear between $a$ and $b$. We use two choices of buffer zones: $a = -0.1, b = 0.1$; $a = -0.05, b = 0.05$ respectively.

On the different figures, the kinetic solution $\rho = u + v$ is plotted with a solid line, while the density of the coupling model $\rho = \rho_L + \rho_R$ is shown by the symbol 'o'. We also plot the exact solution for the full hydrodynamic limit - that is Burgers equation in this case - with dash-dotted line. The buffer zone is made clearly visible by two vertical dotted lines at $x = a$ and $x = b$.

We consider two tests corresponding to two different initial conditions for $\rho$:

(a) uniform: $\rho = 1$;

(b) shock wave: $\rho = 1$ in $[0, 0.5]$ and $\rho = 0.5$ in $[0.5, 1]$.

We compute both transient and steady state solutions.

We explained in example 3.3 that this coupling model cannot preserve uniform flows: this is observed with data (a) in figures 1 and 2. At time $t = 0.0225$ (fig. 1), there is an oscillation in the buffer zone. Then this oscillation is propagated outside the domain, but at the steady state, there remains an oscillation at $x = b$ (fig. 2). This oscillation becomes larger as the length $b - a$ becomes smaller.

For the shock wave, the numerical solution seems to be not very accurate for $t \leq 0.0450$ (figure 3), and when the wave leaves the buffer zone ($t = 0.3150$, figure 4), we again observe an oscillation inside, whereas the solution should be constant there. Again, this oscillation is as large as the length $b - a$ is small. Its influence outside the buffer zone is clearly visible for the narrow buffer zone. We have observed the same phenomenon for a rarefaction wave.

As expected, these tests show that a coupling model that does not preserve uniform flows cannot accurately approximate the original kinetic model.

**Example 6.2.** Numerical solution of the coupling for the 1D BGK model.

Here we test the coupling model for the following BGK model of rarefied gas dynamics, written in the dimensionless form:

$$\partial_t \begin{pmatrix} F \\ G \end{pmatrix} + v\partial_x \begin{pmatrix} F \\ G \end{pmatrix} = \frac{\nu(\rho)}{\varepsilon} \begin{pmatrix} M[\rho] - F \\ \theta M[\rho] - G \end{pmatrix},$$

where $M[\rho] = \frac{n}{\sqrt{2\pi\theta}} \exp(-\frac{(v-u)^2}{2\theta})$ and

$$\rho = (n, nu, n\frac{u^2}{2} + \frac{3}{2}n\theta) = \langle (1, v, \frac{1}{2}v^2)F + (0, 0, 1)G \rangle.$$

The collision frequency is $\nu(\rho) = \frac{\mu}{p}$, where $p = n\theta$ is the pressure and $\mu = \theta^{0.81}$ is the viscosity.

This model is 1D in space and 2D in velocity, but it accounts for 3D velocity effects. It is obtained with standard reduction technique of the full 3-dimensional BGK model of rarefied gas dynamics (see [5]). It is of the form (1), and its hydrodynamic limit is the Euler system of gas dynamics. A coupling model of form (14-15) can be derived, and it can be shown that it preserves uniform flows.

First, we use the classical Sod problem, with the following initial data for density $n$, velocity $u$, and pressure $p$:

$$(n, u, p) = \begin{cases} (1, 0, 1) & -1 \leq x \leq 0 \\ (0.125, 0, 0.1) & 0 \leq x \leq 1 \end{cases}$$

The function $h$ is defined piecewise linear: 0 for $x \leq a$, 1 for $x \geq b$, and linear between $a$ and $b$. We use two choices of buffer zone: $a = 0, b = 0.125$; $a = -0.125, b = 0.125$ respectively. We also use a Heaviside function $h$ that makes the buffer zone reduce to the interface $x = 0$. The Knudsen number $\varepsilon$ is $2 \times 10^{-4}$.

To avoid numerical artifacts in the following comparison, we use a velocity grid of 100 points with bounds [-4,5.4], and a space grid of 10000 points. Such a fine space grid is necessary to make a fair comparison between the models. Indeed, with 300 points only, the numerical dissipation makes the full BGK and the coupling models artificially close.

On the following figures, we plot the numerical solutions for the density and the velocity for the coupling model (solid line), full BGK model (dotted line), and full Euler system (dash-dotted line). The buffer zone is made clearly visible by two vertical dotted lines at $x = a$ and $x = b$ (only one at $x = a$ for the case with Heaviside $h$). The BGK model is solved with a scheme similar to that developed in [12, 13], and the Euler system is solved with a kinetic scheme using the same flux splitting as in the hyperbolic part of the coupling model.

On figure 5, we plot the results obtained with the first buffer zone, at $t = 0.04$. The coupling model is closer to the BGK model than to the Euler solution in the buffer. For $x \leq a$, there is an oscillation in the coupling model which changes from the BGK to the Euler curve. This suggests that the buffer zone is too narrow. At time $t = 0.2$ (figure 6), there is still this oscillation, but the coupling model now is very close to the BGK model in the buffer and in the right part. Note that, as expected, when the BGK model is uniform away from the shock, this property is well preserved by the coupling model

With the second (wider) buffer zone, at $t = 0.04$ (figure 7), the solution lies inside the buffer, and the coupling and BGK models are in almost perfect agreement. At $t = 0.2$ (figure 8), this is also true, even outside the buffer zone and in particular in the left part. Note that there is no oscillation with this buffer.

On figures 9 and 10, the results obtained with the Heaviside function $h$ are plotted at the same times. Surprisingly, there is no oscillation at the interface, as opposed to the case with the narrow buffer zone (figure 5). This suggests that the oscillation is induced by the transition from the Euler to the coupled model, rather than by the transition from Euler to BGK. Apart from this fact, we observe that the results are very close to each model in their respective zones.

Consequently, it seems that the most accurate results (that is the results that are the closest to the full kinetic model) are obtained with the wide buffer zone.

**Example 6.3.** Numerical solution of the coupling for the 2D BGK model.

With this test, we compute the unsteady shock wave produced by the diffraction of a plane moving shock wave that impinges upon a circular cylinder in a rarefied gas.

We point out that our goal here is not to make an accurate comparison between the coupling and the full BGK model. Actually, the mesh we use is too coarse to make a fair comparison: the numerical diffusion makes the results artificially close. In addition, our buffer zone is not well suited to capture the non-equilibrium effects, since the shock rapidly leaves the kinetic zone. However, we believe this test can illustrate the ability of our method to easily treat 2D flows with arbitrary buffer zones.

The data of this computation are taken from [21]. The initial position of the shock is located at $x = -1$. The initial conditions of the undisturbed right state are (in non-dimensionalized form) $n = 1$, $u_x = 0$, $u_y = 0$, $\theta = 1$. The conditions ahead of the moving shock (left state) are given by the Rankine-Hudoniot conditions. The Knudsen number is 0.005 based on the radius of the cylinder equal to 1. The shock Mach number is 2.81 (based on the shock speed and the temperature of the left state), and the wall temperature of the cylinder is $\theta = 1$. A diffuse reflection is used on this wall. Due to the symmetry, only the half plane is computed and symmetry boundary conditions were enforced. The space mesh is a curvilinear grid of $90 \times 90$ cells. The velocity grid is $10 \times 10$ points. Finally, the buffer zone is defined by three rectangles given by the following points: $(-0.6, 0), (-1.3, 0), (-1.3, 2.3), (3.3, 2.3), (3.3, 0), (2.6, 0), (2.6, 1.6), (-0.6, 2.6)$. The kinetic zone lies between the buffer and the cylinder, the hydrodynamic zone lies between the buffer and the exterior of the domain.

On figures 11-13, we plot the density contours for the coupling model (continuous lines) and the full BGK model (dotted lines) at six different times. The buffer zone is plotted with dashed lines. Although the mesh is quite coarse, several shocks can be identified on this figures (primary incident shock, reflected bow shock, Mach shock behind the cylinder, etc.). Moreover, the results of the coupling and the full BGK model are very close.

Note that since the buffer zone is defined by straight lines, it is not aligned with the mesh. Such an interface would be difficult to treat with coupling techniques by interface half-flux conditions (see [15, 17]), while with our method, it does not require any particular treatment. As explained in section 5.2, the geometry of the buffer zone is taken into account by the function $h$ itself in the model.

# 7 Conclusion

In this work, we have proposed a new method to couple kinetic and hydrodynamic equations. This method is an extension of a previous method proposed in [3] for coupling kinetic and diffusion equations. Its main feature is that the two models are coupled in a small buffer zone in which the true solution is approximated by adding up the solutions of each model. The advantage of this coupling is that no boundary condition is needed, as is for a typical domain decomposition method. This makes our method easy to use, since the geometry of the interface is taken into account by the transition function itself in the equations. To implement our method, there is no need to define logically different subdomains: we only need to define the computational grid and a transition function which will be evaluated on the grid. For instance, although it is not done in this paper, several kinetic subdomains with non-connex buffer zones could easily be used without modifying the implementation.

This work is just a first step towards a complete coupling strategy, and an intensive series of numerical tests should be done to measure the performances of our method. But already, we have presented several tests in 1 and 2 space dimensions that show our method behaves quite satisfactorily. We also mention that the kinetic and hydrodynamic zones were fixed *a priori* in our tests, but it is also possible to use a physical criterion to determine the "optimal" zones, as it has already be done for instance in [17, 19]

An important feature of our approach is that it preserves uniform flows for kinetic models which have equilibrium states that are homogeneous functions of degree one with respect to their moments. This property is satisfied by important models as Boltzmann like equations. We have shown that if this property is not satisfied, then the method gives an incorrect approximation of the original kinetic solution.

We also think our method could be extended to a coupling method with moving interfaces. In this paper, we have derived the corresponding coupling model, but the numerical tests are still to be done. In this case, the main problem will be to define how the transition function should evolve in time. There exist a few cases in neutron transport or radiative transfer where the evolution of the interface is known *a priori*. But in some others, as in aerodynamics, other investigations are probably necessary. This will be the subject of an ongoing project by the authors.

# References


[1] J.-F. Bourgat, P. Le Tallec, and M. D. Tidriri. Coupling Boltzmann and Navier-Stokes equations by friction. *J. Comput. Phys*, 127:227–245, 1996.

[2] F. Coron. Derivation of slip boundary conditions for the Navier-Stokes system from the Boltzmann equation. *J. Statist. Phys.*, 54(3-4):829–857, 1989.

[3] P. Degond and S. Jin. A smooth transition model between kinetic and diffusion equations. to appear in Siam J. Numer. Anal., 2004.

[4] F. Golse, S. Jin, and C. D. Levermore. A domain decomposition analysis for a two-scale linear transport problem. *M2AN Math. Model. Numer. Anal.*, 37(6):869–892, 2003.

[5] A. B. Huang and P. F. Hwang. Test of statistical models for gases with and without internal energy states. *Physics of Fluids*, 16(4):466–475, 1973.

[6] S. Jin and Z. P. Xin. The relaxation schemes for systems of conservation laws in arbitrary space dimensions. *Comm. Pure Appl. Math.*, 48(3):235–276, 1995.

[7] A. Klar. Convergence of alternating domain decomposition schemes for kinetic and aerodynamic equations. *Math. Methods Appl. Sci.*, 18(8):649–670, 1995.

[8] A. Klar. Domain decomposition for kinetic problems with nonequilibrium states. *European J. Mech. B Fluids*, 15(2):203–216, 1996.

[9] A. Klar. Asymptotic analysis and coupling conditions for kinetic and hydrodynamic equations. *Comput. Math. Appl.*, 35(1-2):127–137, 1998.

[10] A. Klar, H. Neunzert, and J. Struckmeier. Transition from kinetic theory to macroscopic fluid equations: a problem for domain decomposition and a source for new algorithms. *Transport Theory Statist. Phys.*, 29(1-2):93–106, 2000.

[11] Randall J. LeVeque. *Numerical methods for conservation laws*. Lectures in Mathematics ETH Zürich. Birkhäuser Verlag, Basel, 1990.

[12] L. Mieussens. Discrete Velocity Model and Implicit Scheme for the BGK Equation of Rarefied Gas Dynamics. *Math. Models and Meth. in Appl. Sci.*, 8(10):1121–1149, 2000.

[13] L. Mieussens. Discrete-velocity models and numerical schemes for the Boltzmann-BGK equation in plane and axisymmetric geometries. *J. Comput. Phys.*, 162:429–466, 2000.

[14] Benoît Perthame. *Kinetic formulation of conservation laws*, volume 21 of *Oxford Lecture Series in Mathematics and its Applications*. Oxford University Press, Oxford, 2002.

[15] Y. Qiu. *Étude des équations d'Euler et de Boltzmann et de leur couplage. Application à la simulation numérique d'écoulements hypersoniques de gaz raréfiés*. Institut National de Recherche en Informatique et en Automatique (INRIA), Rocquencourt, 1993. Thèse, Université Paris VI, Paris, 1993.

[16] J. Schneider. Direct coupling of fluid and kinetic equations. *Transport Theory Statist. Phys.*, 25(6):681–698, 1996.

[17] P. Le Tallec and F. Mallinger. Coupling Boltzmann and Navier-Stokes equations by half fluxes. *J. Comput. Phys.*, 136(1):51–67, 1997.

[18] M. Tidriri. Rigorous derivation and analysis of coupling of kinetic equations and their hydrodynamic limits for a simplified Boltzmann model. *J. Statist. Phys.*, 104(1-2):255–290, 2001.

[19] S. Tiwari. Coupling of the Boltzmann and Euler equations with automatic domain decomposition. *J. Comput. Phys.*, 144(2):710–726, 1998.

[20] A. Yamnahakki. Second order boundary conditions for the drift-diffusion equations of semiconductors. *Math. Models Methods Appl. Sci.*, 5(4):429–455, 1995.

[21] J.Y. Yang and J.C. Huang. Rarefied Flow Computations Using Nonlinear Model Boltzmann Equations. *Journal of Computational Physics*, 120:323–339, 1995.

[22] H. C. Yee. *A Class of High-Resolution Explicit and Implicit Shock-Capturing Methods*. von Karman Institute for Fluid Dynamics, Lectures Series, n$^o$4. 1989.

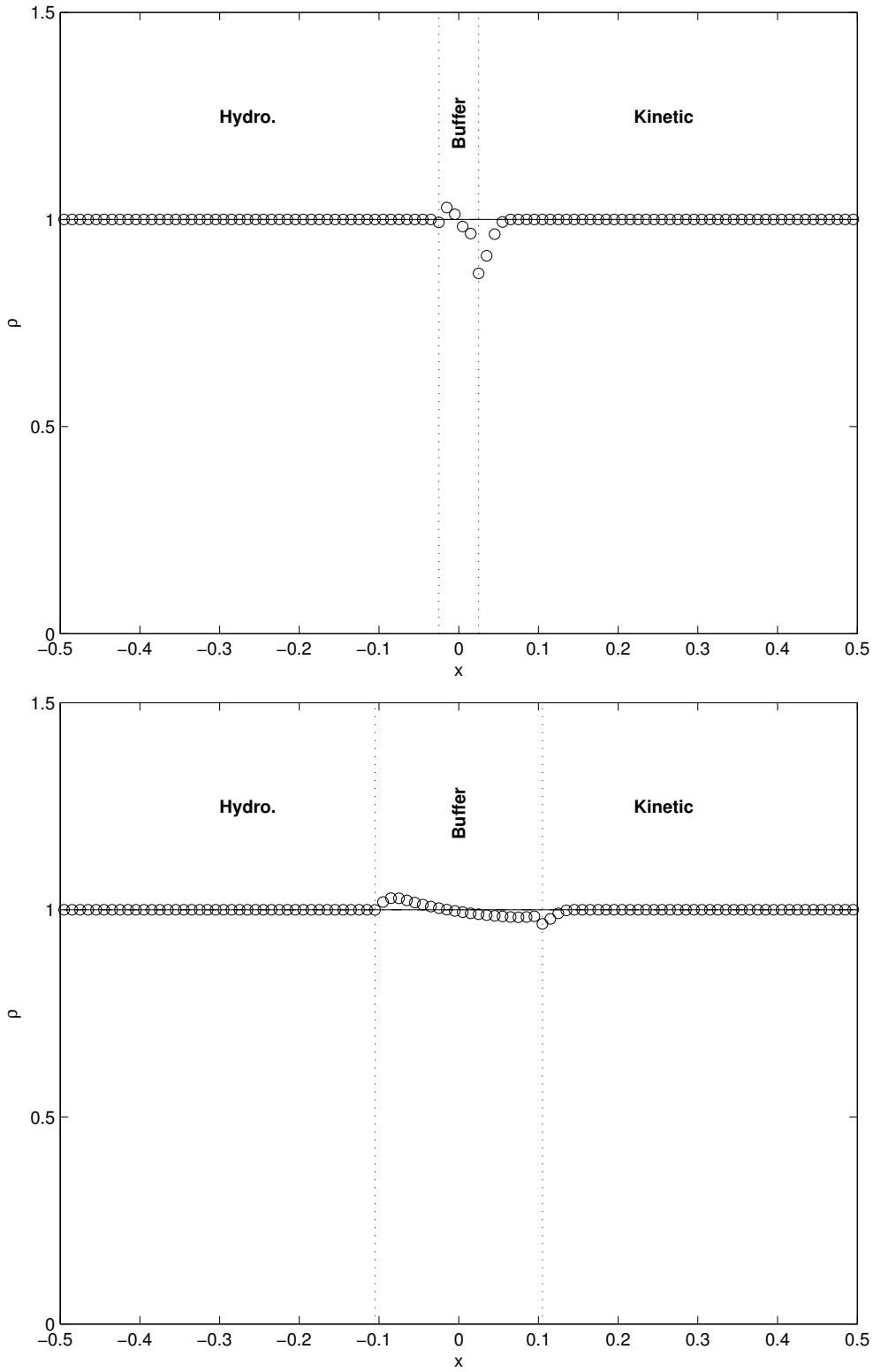


Figure 1: The numerical solution of $\rho$ for the Jin-Xin relaxation model (18) at $t = 0.025$ for the uniform initial condition, with narrow (top) and large (bottom) buffer zone. The solid line is the (constant) solution of model (18), while 'o' is the numerical solution of the coupling model with 100 grid points.

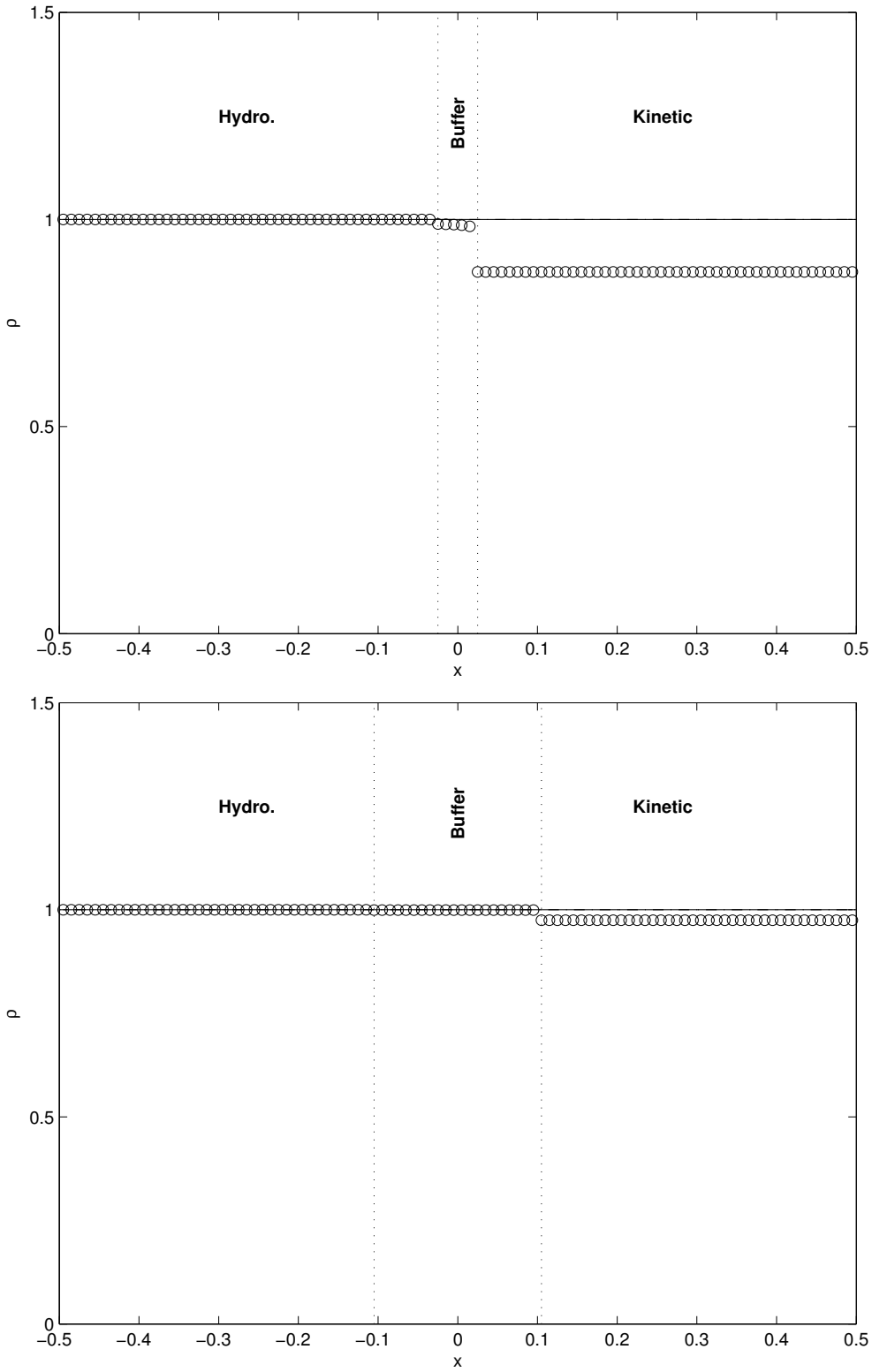


Figure 2: The numerical solution of $\rho$ for the Jin-Xin relaxation model (18) at steady state for the uniform initial condition, with narrow (top) and large (bottom) buffer zone. The solid line is the (constant) solution of model (18), while 'o' is the numerical solution of the coupling model with 100 grid points.

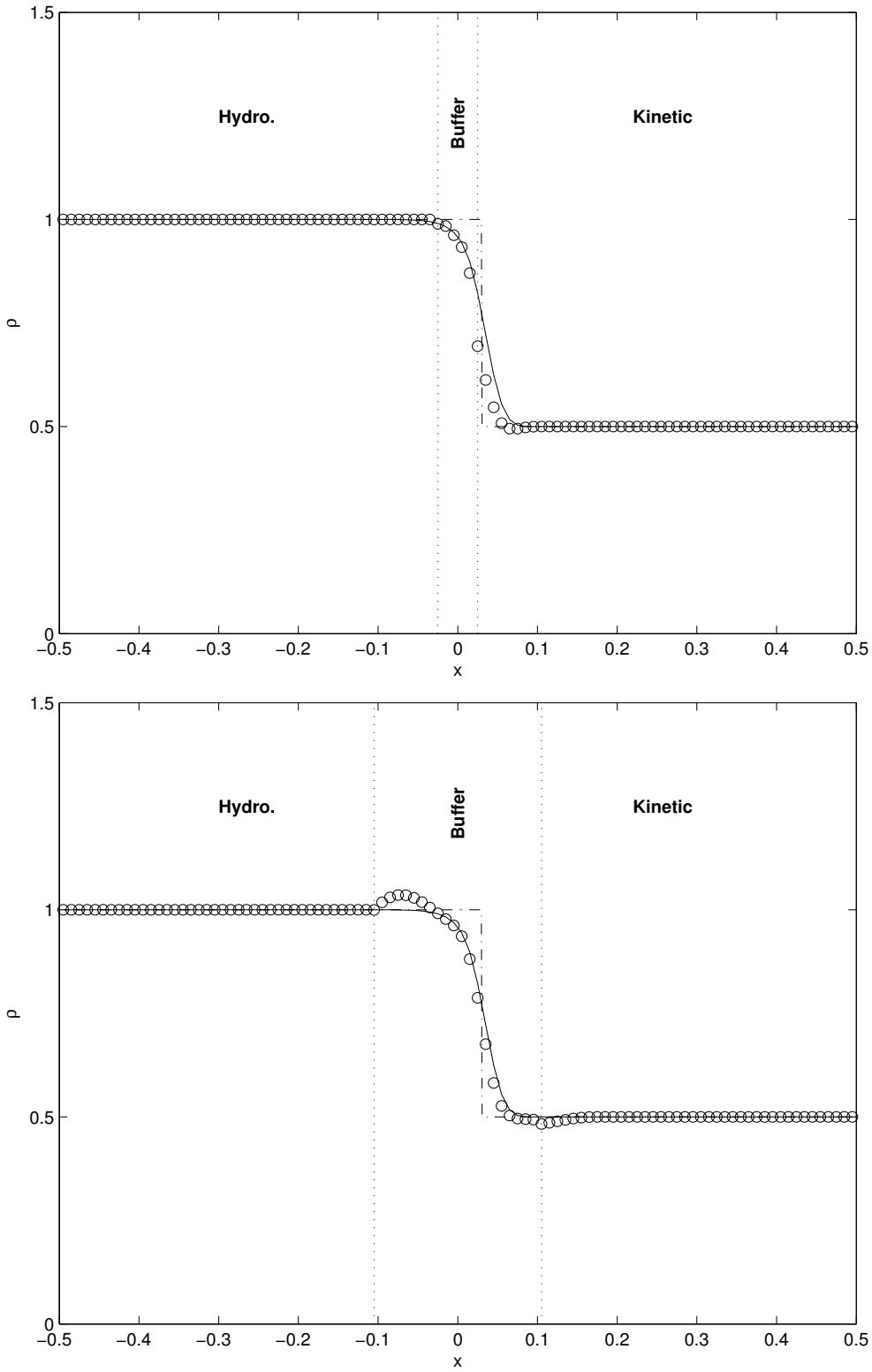


Figure 3: The numerical solution of $\rho$ for the Jin-Xin relaxation model (18) at $t = 0.0450$ for the shock initial condition, with narrow (top) and large (bottom) buffer zone. The solid line is the numerical solution of model (18), while 'o' is the numerical solution of the coupling model (100 grid points), and '.-' is the exact solution for the Burgers equation (full hydrodynamic limit).

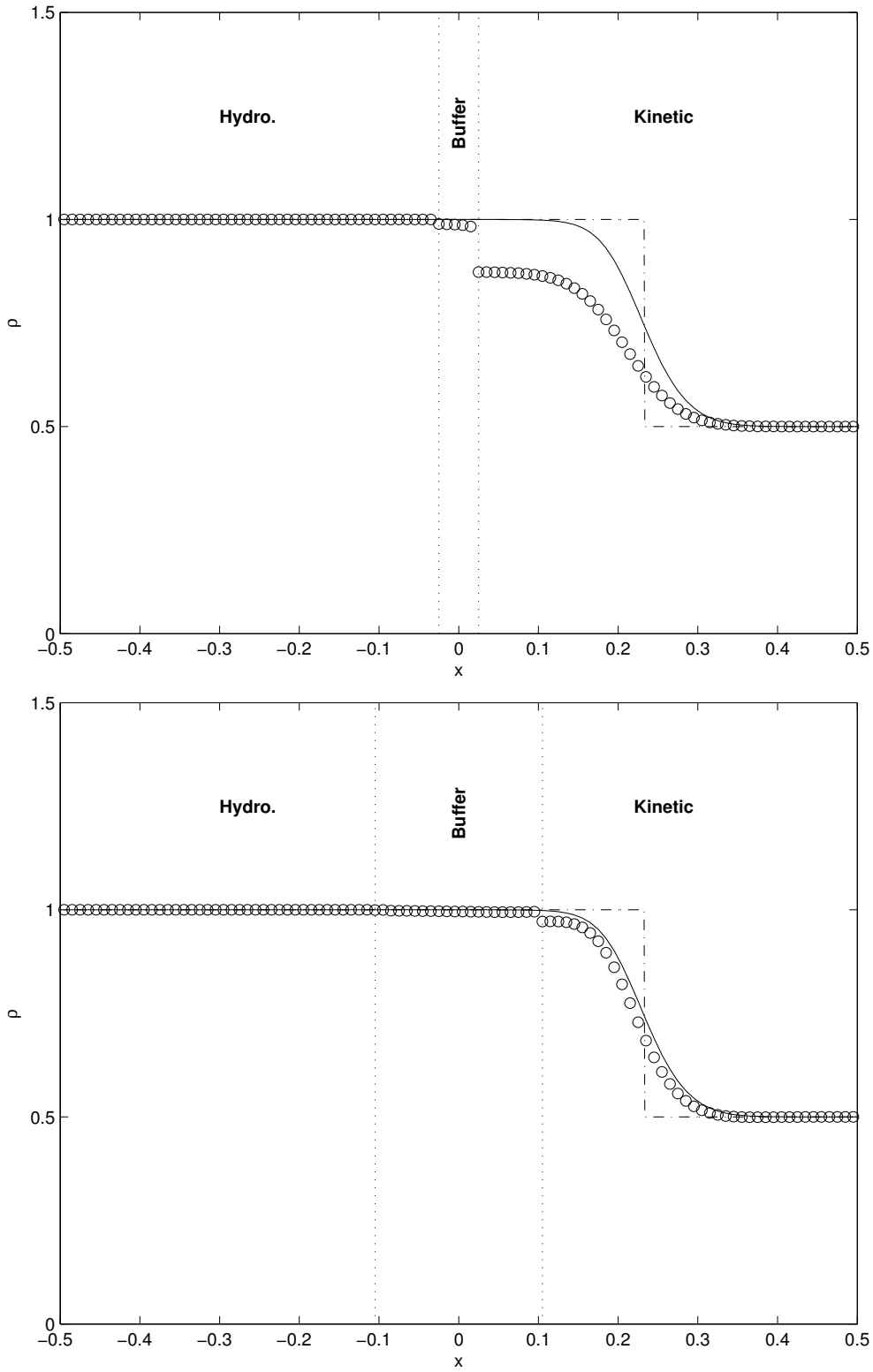


Figure 4: The numerical solution of $\rho$ for the Jin-Xin relaxation model (18) at $t = 0.3150$ for the shock initial condition, with narrow (top) and large (bottom) buffer zone. The solid line is the numerical solution of model (18), while 'o' is the numerical solution of the coupling model (100 grid points), and '.-' is the exact solution for the Burgers equation (full hydrodynamic limit).

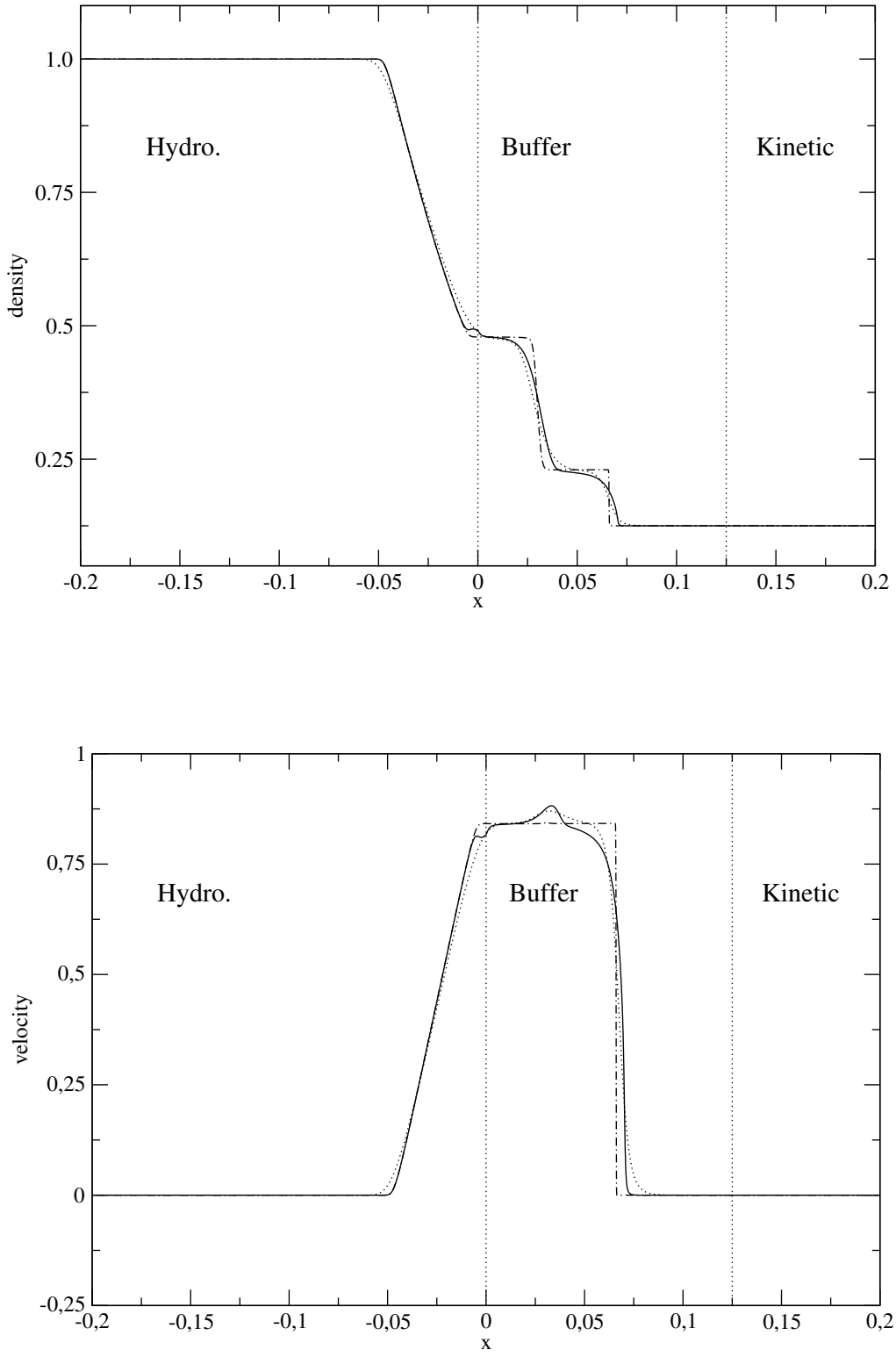


Figure 5: The numerical solution of density (top) and velocity (bottom) for the BGK model at $t = 0.04$ for the Sod problem (buffer $[0, 0.125]$). The solid line is the solution of the coupling model, the dotted line is the BGK model, while the dot-dashed line is the Euler system.

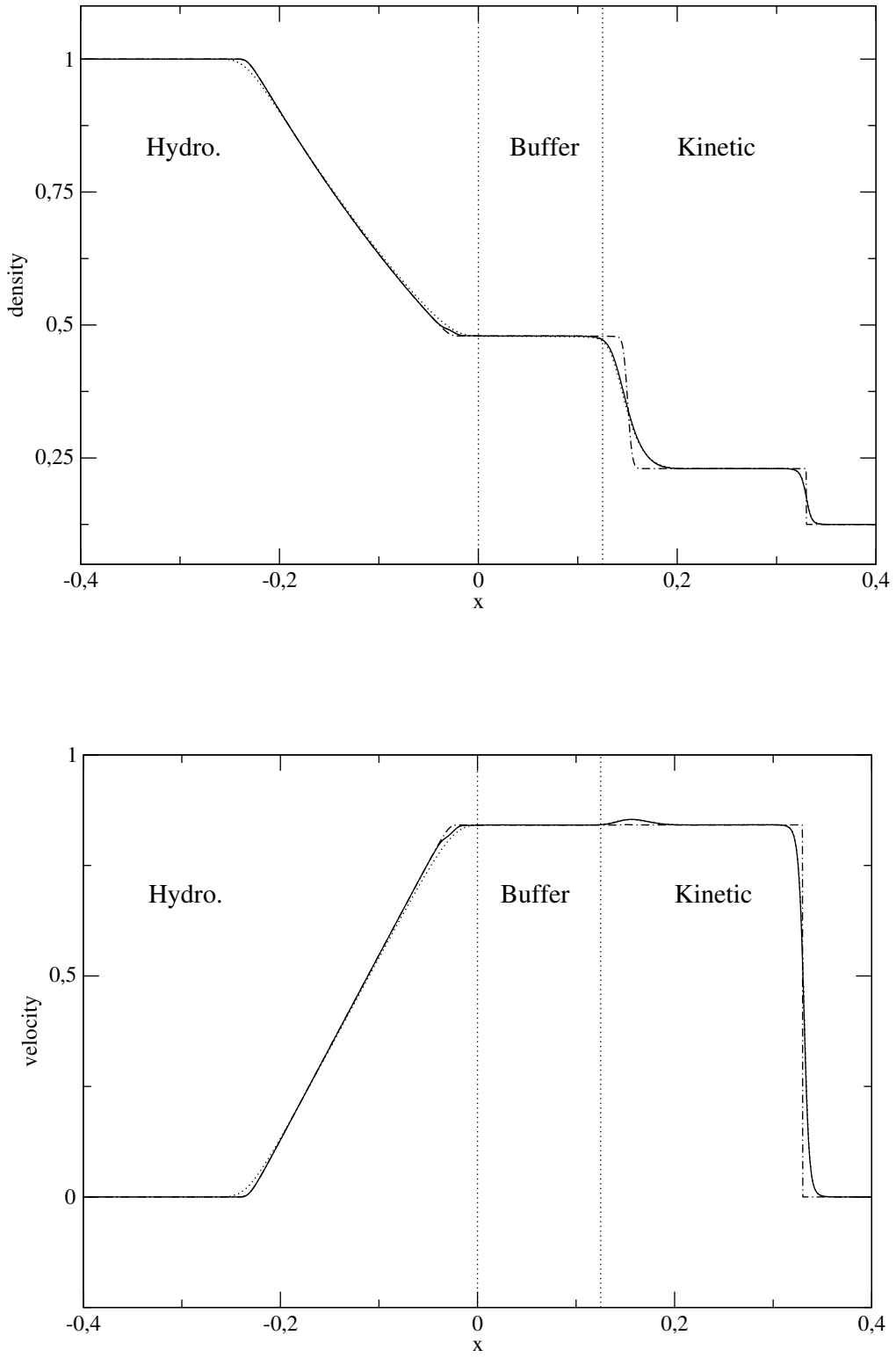


Figure 6: The numerical solution of density (top) and velocity (bottom) for the BGK model at $t = 0.2$ for the Sod problem (buffer $[0, 0.125]$). The solid line is the solution of the coupling model, the dotted line is the BGK model, while the dot-dashed line is the Euler system.

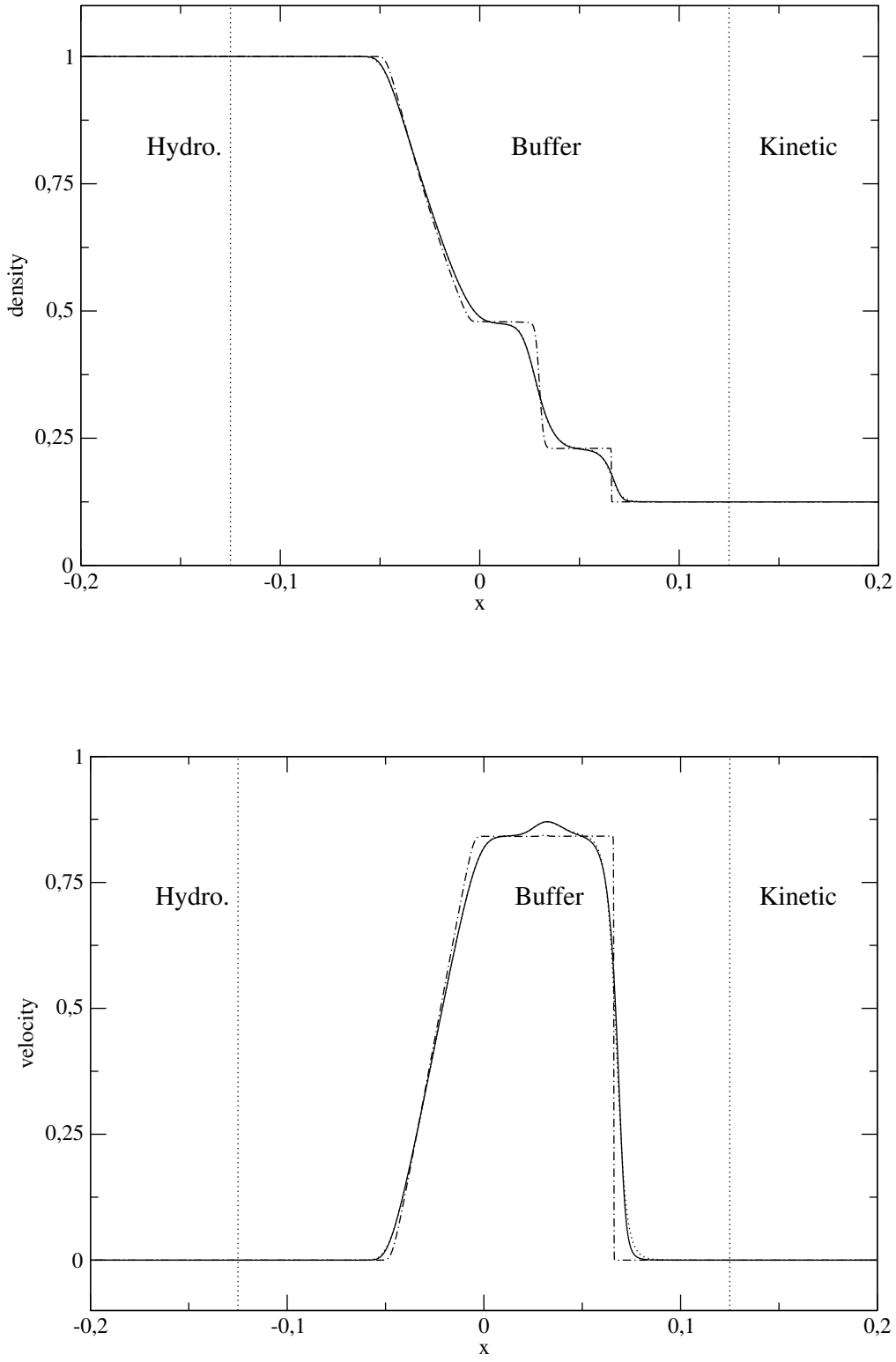


Figure 7: The numerical solution of density (top) and velocity (bottom) for the BGK model at $t = 0.04$ for the Sod problem (buffer $[-0.125, 0.125]$). The solid line is the solution of the coupling model, the dotted line is the BGK model, while the dot-dashed line is the Euler system.

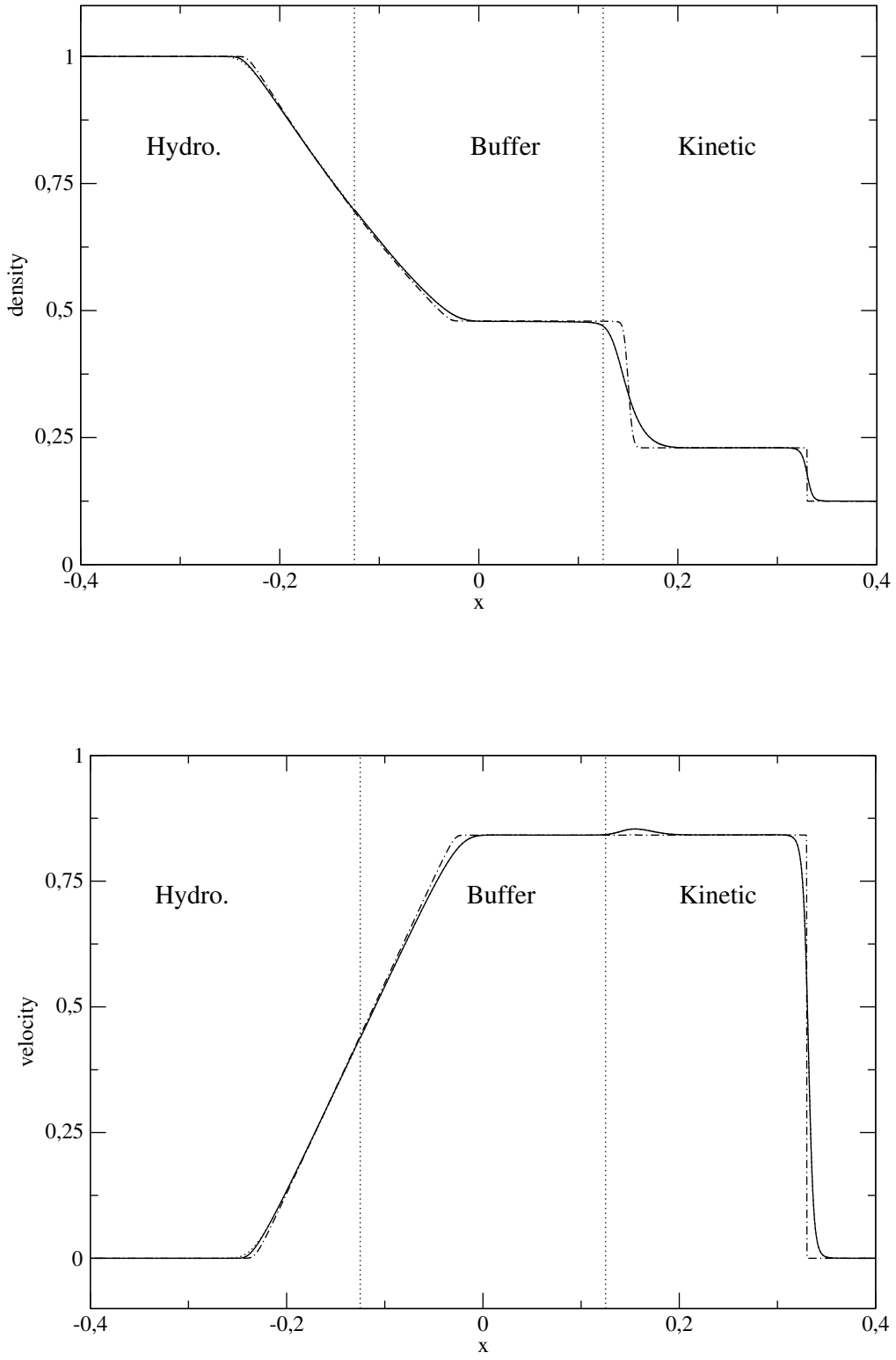


Figure 8: The numerical solution of density (top) and velocity (bottom) for the BGK model at $t = 0.2$ for the Sod problem (buffer $[-0.125, 0.125]$). The solid line is the solution of the coupling model, the dotted line is the BGK model, while the dot-dashed line is the Euler system.

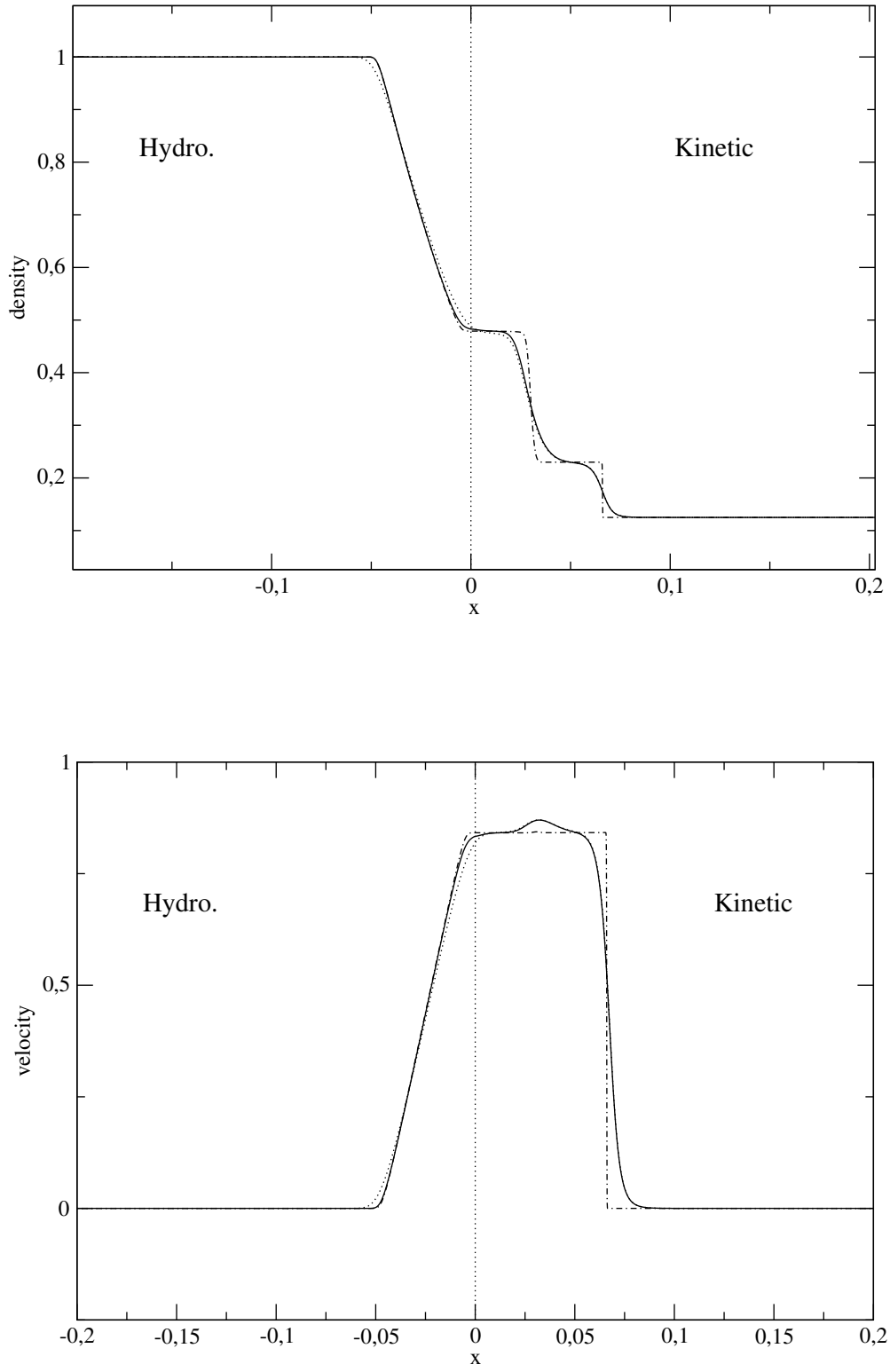


Figure 9: The numerical solution of density (top) and velocity (bottom) for the BGK model at $t = 0.04$ for the Sod problem (buffer reduced to the interface $x = 0$ with the Heaviside function). The solid line is the solution of the coupling model, the dotted line is the BGK model, while the dot-dashed line is the Euler system.

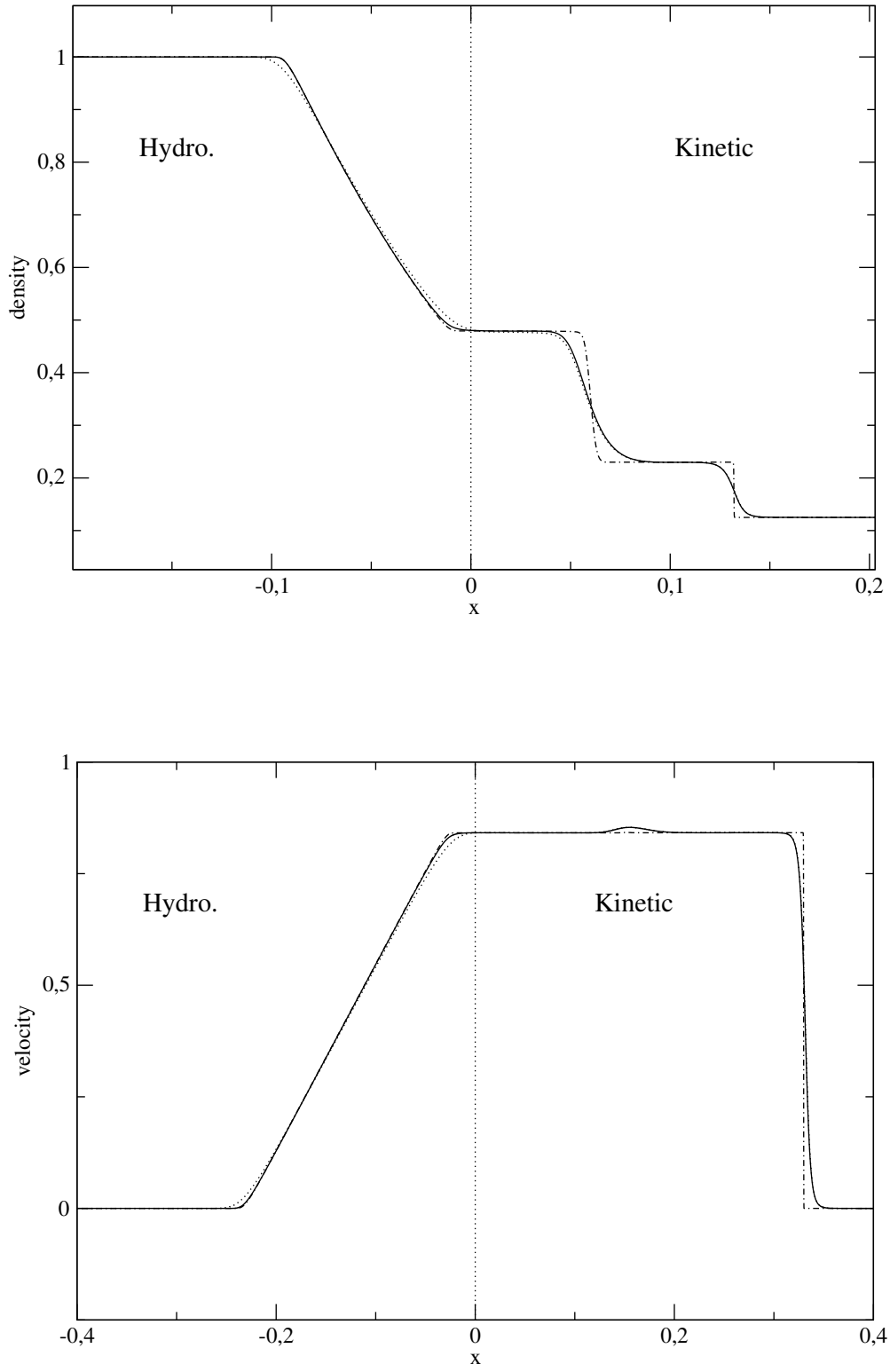


Figure 10: The numerical solution of density (top) and velocity (bottom) for the BGK model at $t = 0.2$ for the Sod problem (buffer reduced to the interface $x = 0$ with the Heaviside function). The solid line is the solution of the coupling model, the dotted line is the BGK model, while the dot-dashed line is the Euler system.

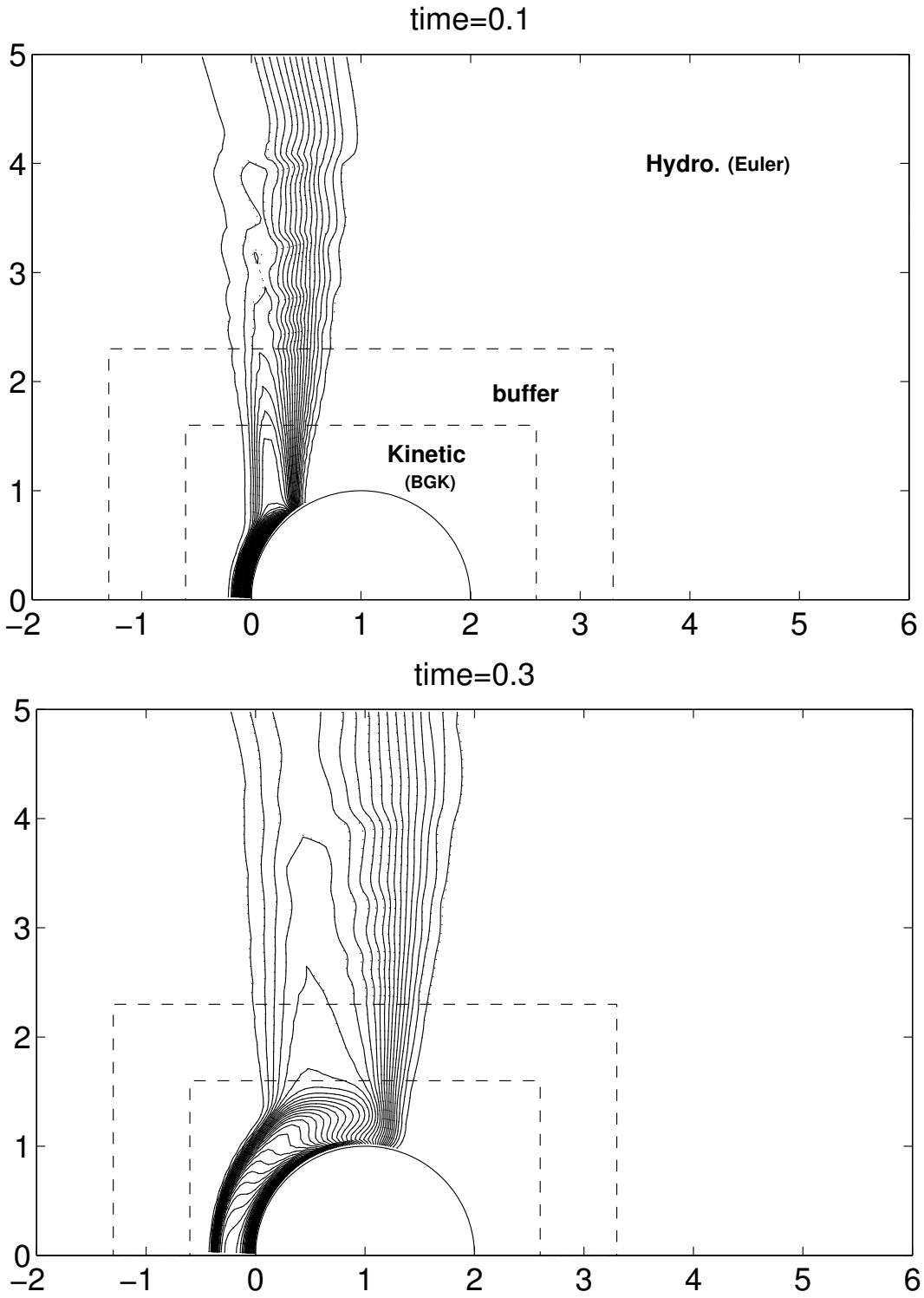


Figure 11: Shock diffraction around a circular cylinder in a rarefied gas, with Knudsen=0.005 and Mach shock=2.81. Density contours at different times for the coupling model (continuous lines) and the BGK model (dotted lines). The buffer zone is between the dashed lines. The function $h$ is 1 in the zone close to the cylinder (kinetic), 0 in the exterior domain (hydrodynamic), and between 0 and 1 in the buffer zone.

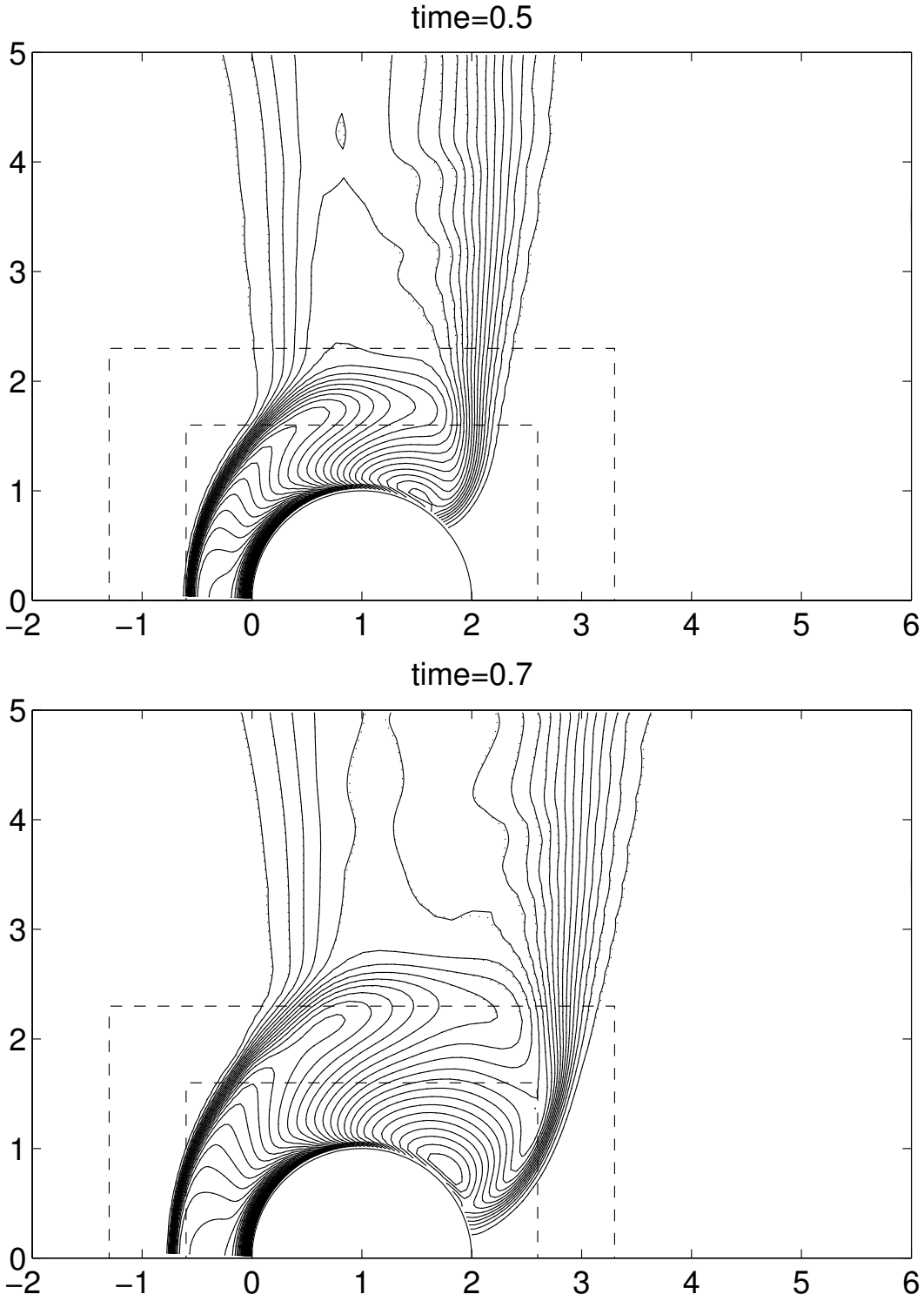


Figure 12: sequel of fig. 11

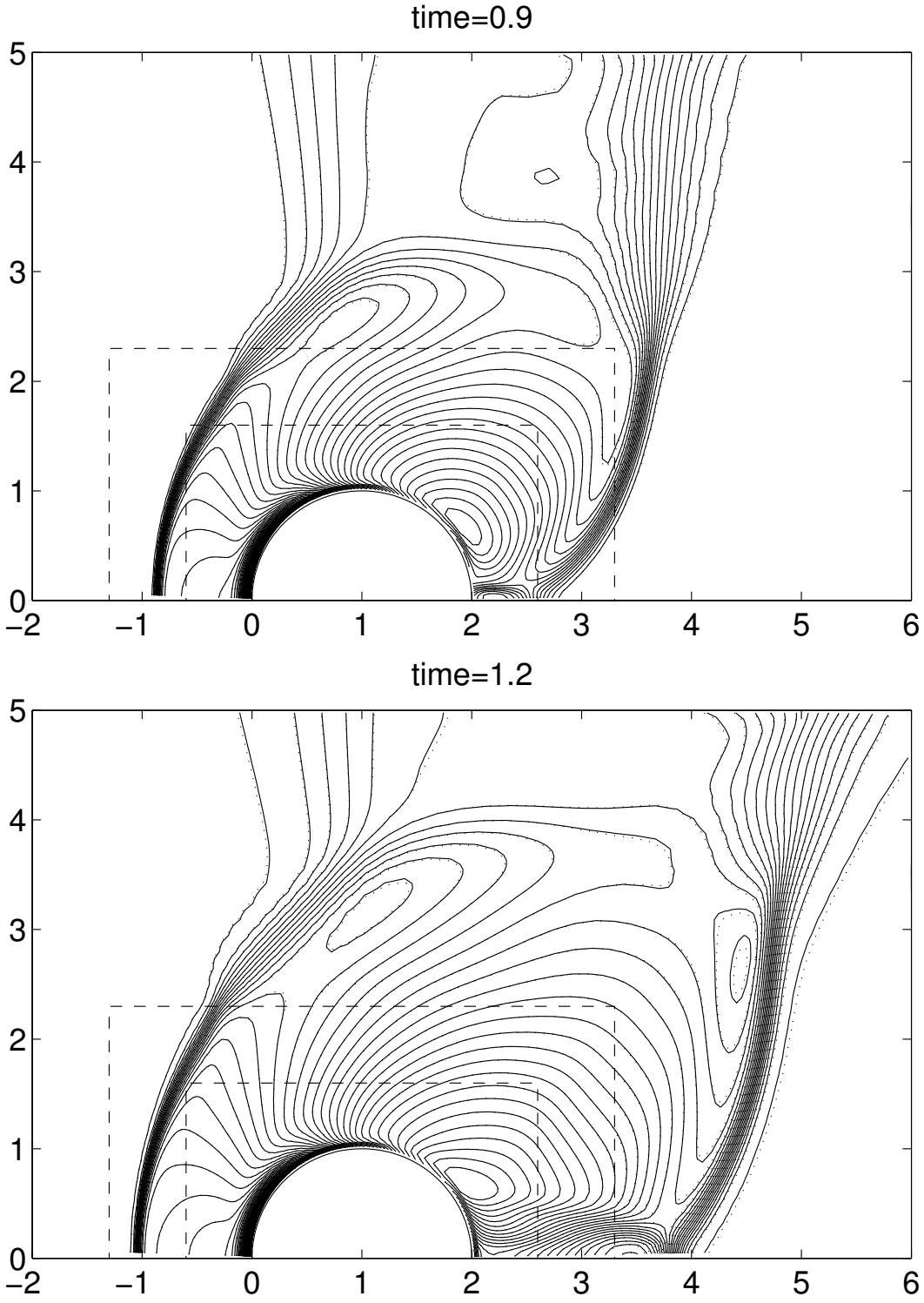


Figure 13: sequel of fig. 12